Aalborg Universitet

On the Manufacturing Processes of Flexible Thermoelectric Generators

Mortazavinatanzi, Seyedmohammad

ON THE MANUFACTURING PROCESSES OF FLEXIBLE THERMOELECTRIC GENERATORS

BY
SEYEDMOHAMMAD MORTAZAVINATANZI

DISSERTATION SUBMITTED 2021

AALBORG UNIVERSITY

DENMARK

ON THE MANUFACTURING PROCESSES OF FLEXIBLE THERMOELECTRIC GENERATORS

PH.D. DISSERTATION

Seyedmohammad Mortazavinatanzi

Department of Energy Technology
Aalborg University, Denmark

Dissertation submitted December 2020

CV

Seyedmohammad Mortazavinatanzi received his B.Sc. degree in Manufacturing Engineering from Mazandaran University, Babol, Iran, in 2005, and his M.Sc. in Manufacturing Engineering from AmirKabir University of Technology, Tehran, Iran, in 2009.

He is currently pursuing his study to obtain his Ph.D. degree in the Department of Energy Technology, Aalborg University, Denmark. He co-founded the spin-off company, ParsNord Thermal Comfort ApS funded by the innovation fund Denmark during the last year of his Ph.D. study. His research interests include thermoelectric device manufacturing, additive manufacturing, printed electronics, flexible hybrid electronics, thermoelectric cooling/heating, waste heat recovery, and renewable energy.

ENGLISH SUMMARY

It has been widely accepted among the scientific community that the rising greenhouse gas level is the main contributor to global warming. Greenhouse gases reduction by 20% compared to 1990 or by 30% (if all the countries involved are committed to playing the roles equally) as well as enhancing the share of the renewable source of energy to 20% in the overall energy consumption are the major objectives of the Paris climate agreement in 2015. The main contributors to the increasing trend of greenhouse gases are power plants and fossil fuel consumption. Nevertheless, a significant portion of the generated energy is released in the surrounding environment in waste heat, both in the industry, residential and transportation sectors. The amount of waste heat also significantly large for the transportation sector (60% energy loss). Generally speaking, only 20% of the global energy consumption is converted to effective work, while the rest is lost in the form of waste heat.

Thermoelectric devices are solid-state technology that can convert waste heat into useful electricity. They generate a voltage potential upon applying a temperature difference across them. Commercial thermoelectric devices typically consist of arrays of semiconductor materials sandwiched between the two parallel electrical insulative sheets. Their solid-state nature introduces them as reliable solutions for waste heat recovery applications compared to other techniques such as the organic Rankine cycle (ORC) based waste heat recovery. Besides, thermoelectric devices can be utilized for direct electrical energy generation by imposing them on a renewable source of heat energy, such as solar radiation. In this case, the device is called a solar thermoelectric generator (STEG), which can be considered a sustainable solution for solar energy conversion.

Despite the mentioned advantages, the low efficiency of the thermoelectric materials, high material cost, and lack of a scalable manufacturing method have been the main barriers to the widespread utilization of thermoelectric devices. There have been many attempts to develop efficient and low-cost thermoelectric materials. until now, bismuth telluride has shown the best thermoelectric energy conversion efficiency at room temperatures (4% to 7%). This relatively low performance is not sufficient for current commercial thermoelectric material to be adopted for large scale industrial waste heat recovery. It is also worth mentioning that the most efficient thermoelectric materials contain rare earth elements that can lead to a semiconductor market disruption in large-scale utilization. Consequently, any effort in material development research should be in the direction of finding new materials that are earth-abundant to solve the material scarcity problem.

On the other hand, finding inexpensive and efficient thermoelectric material does not tackle integrating these materials into a final applicable device. In other words, the lack of scalable manufacturing methods for high-throughput fabrication of thermoelectric devices leads to the high cost of thermoelectric systems and limitations in the areas of applications. In this Ph.D. thesis, one of the main goals is to develop a new manufacturing concept for industrial-scale automated manufacturing of thermoelectric devices. The high-throughput fabrication results in lowering the total thermoelectric system cost and availability for large volume applications. The commercial thermoelectric devices are also fabricated in small sizes and non-flexible structure (rigid). Besides, most of the waste heat is emitted from the large area and none flat (curved) surface into the surrounding environment.

Consequently, introducing fabrication methods to bring flexibility to thermoelectric devices has been the focus of many researchers' attempts. These works can be categorized into two different directions: flexible thermoelectric materials development and fabrication of flexible devices through rigid thermoelectric materials. The first category mostly has studied the polymer-based organic thermoelectric materials, which can be applied in printable inks or pastes. Regardless of proving high mechanical flexibility, these groups of materials suffer from low thermoelectric efficiency. In the second direction, the same bulk thermoelectric materials applied in commercial devices have been used in a flexible structure to provide the required level of flexibility. As the main part of this Ph.D. thesis, the same strategy (category two) was chosen to develop a manufacturing platform for automated high-throughput fabrication of flexible thermoelectric devices. The proposed concept is similar to a method called Flexible Hybrid Electronics (FHE), which enables the combination of rigid silicon electronics and printed electronics to provide a flexible printed electronics product. Nano-silver (Ag) bonding also was investigated to bond the bulk thermoelectric materials on top of a flexible substrate. This relatively novel bonding technique, which is increasingly used as the die-attach material in power electronics, shows promising performances compared to the conventional bonding materials for thermoelectric fabrication like low-temperature solder pastes.

Keywords: Thermoelectric Generator (TEG); Flexible Thermoelectric Generators (FTEG); Flexible Hybrid Electronics (FHE); Thermoelectric Modules Manufacturing; Medium Temperature Thermoelectric Generators; Flexible Thin-film Thermoelectric Generators; Nano-silver (Ag) bonding.

DANSK RESUME

Det er bredt accepteret blandt det videnskabelige samfund, at det stigende drivhusgasniveau er den største bidragyder til den globale opvarmning. Reduktion af drivhusgasser med 20% sammenlignet med 1990 eller med 30% (hvis alle de involverede lande er forpligtet til ens mål) samt at øge andelen af den vedvarende energikilde til 20% af det samlede energiforbrug er en af de største målsætninger i Paris-klimaaftalen i 2015. De vigtigste bidragydere til den stigende tendens for drivhusgasser er kraftværker og fossilt brændstofforbrug. Ikke desto mindre frigøres en betydelig del af den genererede energi til det omgivende miljø som spildvarme, både i industrien, boliger og transportsektoren. Mængden af spildvarme er også betydelig for transportsektoren (60% energitab). Generelt konverteres kun 20% af det globale energiforbrug til effektivt arbejde, mens resten går tabt i form af spildvarme.

Termoelektriske enheder er baseret på solid state-teknologi, der kan omdanne spildvarme til nyttig elektricitet ved at generere et spændingspotentiale ud fra temperaturforskellen på tværs af dem. Kommercielle termoelektriske enheder består typisk af arrays af halvledermaterialer, der er klemt mellem to parallelle elektriske isoleringsplader. Deres solid state-natur gør dem til pålidelige løsninger til spildvarmegenvindingsapplikationer sammenlignet med andre teknikker såsom den organiske Rankine-cyklus (ORC). Derudover kan termoelektriske enheder anvendes til direkte elektrisk energiproduktion ved at pålægge dem en vedvarende kilde til termisk energi, såsom solstråling. I dette tilfælde kaldes enheden en sol-termoelektrisk generator (STEG), der kan betragtes som en bæredygtig løsning til konvertering af solenergi.

På trods af de nævnte fordele har den lave effektivitet af de termoelektriske materialer, høje materialepriser og manglen på en skalerbar fremstillingsmetode været de vigtigste barrierer for den udbredte anvendelse af termoelektriske anordninger. Der har været mange forsøg på at udvikle effektive og billige termoelektriske materialer. Indtil nu har bismuth telluride vist den bedste termoelektriske energiomdannelseseffektivitet ved stuetemperatur (4% til 7%). Denne relativt lave ydeevne er ikke tilstrækkelig til, at det nuværende kommercielle termoelektriske materiale kan anvendes til storskala industriel spildvarmegenvinding. Det er også værd at nævne, at de mest effektive termoelektriske materialer indeholder sjældne jordarter, der kan blive en flaskehals for opskalering af halvledermarkedet. Derfor bør enhver indsats inden for forskning i materialeudvikling være i retning af at finde nye materialer, der er rigelige på jorden for at løse det materielle knaphedsproblem.

På den anden side er det ikke kun integration af disse materialer i en endelig anvendelig enhed ved at finde billigt og effektivt termoelektrisk materiale, der har betydning. Manglen på skalerbare fremstillingsmetoder til fremstilling af termoelektriske enheder medvirker til de høje omkostninger ved termoelektriske systemer og begrænsninger inden for anvendelsesområderne. I denne Ph.D. afhandling er et af hovedmålene at udvikle et nyt produktionskoncept til automatiseret industriel produktion af termoelektriske enheder. Fremstillingen med høj kapacitet resulterer i en nedsættelse af de samlede termoelektriske systemomkostninger og tilgængelighed til applikationer med stort volumen. De kommercielle termoelektriske enheder er også fremstillet i små størrelser og ikke-fleksibel struktur (stiv). Desuden udsendes det meste af spildvarmen fra det store område og ingen flad (buet) overflade i det omgivende miljø.

Derfor har introduktion af fabrikationsmetoder til at bringe fleksibilitet til termoelektriske enheder været fokus for mange forskeres forsøg. Disse værker kan kategoriseres i to forskellige retninger: udvikling af fleksible termoelektriske materialer og fremstilling af fleksible enheder gennem stive termoelektriske materialer. Den første kategori har for det meste undersøgt de polymerbaserede organiske termoelektriske materialer, som kan anvendes i trykfarver eller pastaer. Uanset at der påvises høj mekanisk fleksibilitet, lider disse grupper af materialer under lav termoelektrisk effektivitet. I den anden retning er de samme termoelektriske bulkmaterialer anvendt i kommercielle indretninger blevet anvendt i en fleksibel struktur for at tilvejebringe det krævede niveau af fleksibilitet. Som hoveddelen af denne Ph.D. afhandling, blev den samme strategi (kategori to) valgt til at udvikle en fremstillingsplatform til automatiseret fremstilling af højt gennemløb af fleksible termoelektriske enheder. Det foreslåede koncept svarer til en metode kaldet Flexible Hybrid Electronics (FHE), som muliggør kombinationen af stiv siliciumelektronik og trykt elektronik for at give et fleksibelt elektronikprodukt. Nano-sølv (Ag) -binding blev også undersøgt for at binde de termoelektriske bulkmaterialer oven på et fleksibelt substrat. Denne relativt hidtil ukendte bindingsteknik, der i stigende grad anvendes som vedhængsmateriale i kraftelektronik, viser lovende præstationer sammenlignet med de konventionelle bindingsmaterialer til termoelektrisk fremstilling som lodde pasta med lav temperatur.

Nøgleord: Termoelektrisk generator (TEG); Fleksible termoelektriske generatorer (FTEG); Fleksibel hybridelektronik (FHE); Produktion af termoelektriske moduler; Medium-temperatur termoelektriske generatorer; Fleksible tyndfilm termoelektriske generatorer; Nano-sølv (Ag) binding.

PREFACE

This research conducted from January 2017 to December 2020 at Alborg University, Department of Energy Technology is submitted in the form of this dissertation to the Doctoral School of Engineering and Science at Aalborg University in order to obtain the Danish Ph.D. degree. It is provided in the collection of papers format in six chapters. Prof. Lasse Rosendahl and Assoc. Prof. Alireza Rezaniakolaei at the Department of Energy have been the main supervisor and co-supervisor of this research work.

ACKNOWLEDGEMENTS

THESIS DETAIL AND PUBLICATIONS

Thesis Title: On the Manufacturing Processes of Flexible Thermoelectric Generators.

Ph.D. Student: Seyedmohammad Mortazavinatanzi

Supervisor: Prof. Lasse Rosendahl, Aalborg University

Co-supervisor: Assoc. Prof. Alireza Rezaniakolaei, Aalborg University

This dissertation is written on the basis of the following publications, which have been accomplished in the Ph.D. study period. The papers are accessible in the Appendix section of the dissertation.

Publications:

A. S. Mortazavinatanzi, A. Rezaniakolaei, and L. Rosendahl, "Printing and Folding: A Solution for High-Throughput Processing of Organic Thin-Film Thermoelectric Devices," Sensors 2018, Vol. 18, Page 989, vol. 18, no. 4, p. 989, Mar. 2018.

B. S. Mortazavinatanzi, S. Mojtaba Mir Hosseini, L. Song, B. Brummerstedt Iversen, L. Rosendahl, and A. Rezania, "Zinc Antimonide Thin Film Based Flexible Thermoelectric Module," Mater. Lett., vol. 280, p. 128582, Aug. 2020.

C. S. Mortazavinatanzi, A. Rezaniakolaei, and L. Rosendahl, "High-throughput Manufacturing of Flexible Thermoelectric Generators for Low to Medium Temperature Applications Based on Nano-silver Bonding," (*submitted to the IEEE Trans. Electron Devices*).

TABLE OF CONTENTS

CHAPTER 1. INTRODUCTION

The introduction aims to provide an overview of the fundamentals of thermoelectricity, thermoelectric (TE) modules, and applications. Different manufacturing methods are introduced, and their feasibility for thermoelectric device fabrication is discussed. The importance of the mechanical flexibility for a thermoelectric device is explored, and various techniques to achieve this feature are introduced. The chapter is summarized by the project goals and outline of the dissertation.

1.1 INTRODUCTION TO THE THERMOELECTRIC DEVICES

The rapid rise of CO_2 emissions in recent years and boosting global demand for electricity, heating, and cooling imposes significant challenges worldwide. As a result, it is crucial for nations to investigate alternative energy sources to meet the increasing energy demand and to suspend climate change. In this direction, thermoelectric devices could be investigated as an alternative clean electricity generator and heating/cooling solution. When a thermoelectric device is used for power generation, it is called a thermoelectric generator (TEG). TEGs can convert heat fluxes into electricity as long as a temperature difference is applied to the devices. They act as heat engines and operate between a heat source and a heat sink to convert a part of the heat energy into electricity. Like other Carnot cycle based heat engines, it is crucial to maintain the temperature difference across the device to reach the maximum electrical power output. Besides, the thermoelectric material properties directly affect the efficiency of converting waste heat into electricity. This characteristic makes TEGs attractive for harvesting residual energies in the form of waste heat, which are typically released into the surrounding environment. They can generate electricity without any moving part in a reliable manner. Thermoelectric devices also can operate as heat pumps in a reverse direction. With passing a DC electrical current, heat can be pumped across the device, and a temperature difference is generated. In this direction, thermoelectric devices are mostly utilized for cooling applications and typically are called thermoelectric coolers (TECs). Like the generator mode, the cooling effect can be achieved without any moving element, which makes this approach highly reliable. Since there is no refrigerant involved in this process, it is also environmentally friendly compared to the conventional cooling methods containing a refrigerant.

Despite all the mentioned advantages, the main drawback of the vast utilization of thermoelectricity is the low conversion efficiency of the current thermoelectric materials and the high manufacturing cost. Besides, the lack of flexibility in thermoelectric modules, makes it difficult to implement them on large scales containing curved contact surfaces. Many researchers have been focused on overcoming this barrier by introducing novel materials with the help of nanotechnology. In this thesis, the focuse is on introducing innovative manufacturing solutions for scaling up thermoelectricity into a broader range of applications. Such a manufacturing method should handle high throughput production, which leads to decreasing the overall cost of the system and time of the manufacturing. Besides, the proposed manufacturing concepts should be capable of bringing flexibility for thermoelectric modules by utilizing proper flexible substrate and bonding materials.

1.2 FUNDAMENTALS OF THERMOELECTRIC DEVICES

A typical thermoelectric module consists of two different thermoelectric materials, n-type (negatively charged) and p-type (positively charged), which are sandwiched between the two parallel substrates (Figure 1.1). The semiconductor materials usually are in cubic pellets and attached to the substrate by different bonding methods like soldering, silver sintering, and hot pressing. Each substrate contains an electrical insolated sheet which is pre-patterned by electrically conductive interconnectors. These interconnectors form a circuit to connect the thermoelectric pellets in an electrically in series and a thermally in parallel way. Copper bonded ceramics are the most common substrate for commercial thermoelectric devices since the ceramic is a suitable electrical insulator and thermal conductor. When one substrate heats up (hot side) and one becomes cold (cold side), a DC electrical current flows through the device, and the value of this current is directly proportional to the amount of this thermal gradient. In a reverse manner, if a DC electrical current passes through the device, one substrate becomes hot, and the other side gets cold. The device's hot and cold side can be changed conveniently only by reversing the direction of the electrical current. Seebeck, Peltier, and Thomson effects are explained to determine the physics contributed in thermoelectric device functionality in the following sections.
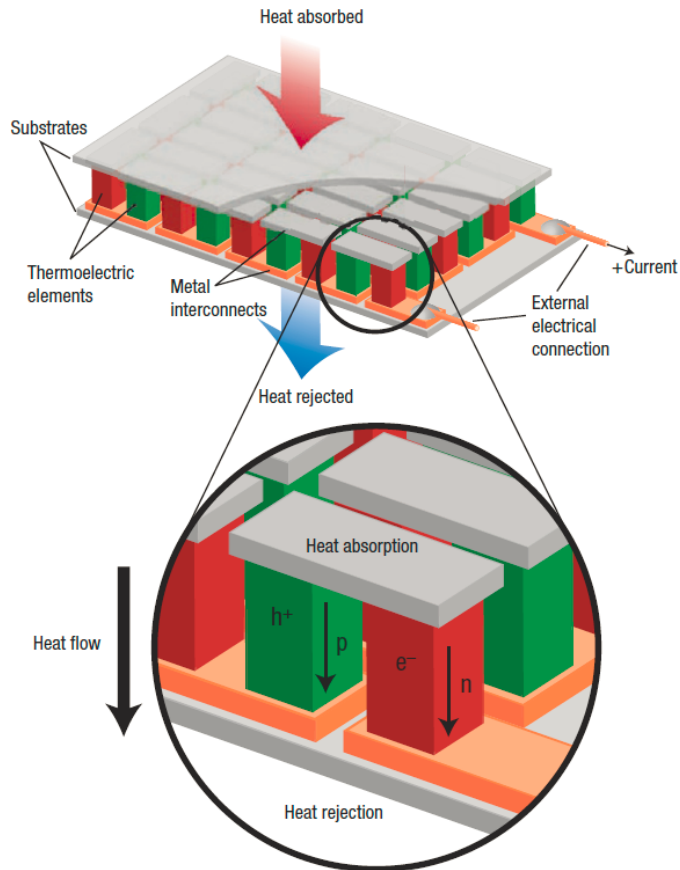
Fig. 1.1: Features of a typical thermoelectric module [1].

1.2.1 SEEBECK EFFECT

The Seebeck effect describes the generation of an electrical thermo-voltage as a result of the existence of a temperature difference between two sides of a thermoelectric device. Based on this effect, which was discovered by Thomas Johann Seebeck in 1821-3, when one of the junctions of two dissimilar conductors or semi-conductors material in a circuit is heated up, a voltage difference is generated [2]. This happens due to the diffusion of charge carriers, which results in moving electrical charges from the hot to the cold side. There are two types of charge carriers (electrons and holes) that determine the type of thermoelectric material (n-

type and p-type). Figure 1.2 shows a circuit consisting of two dissimilar conductors a and b, connected thermally in parallel and electrically in series. When a thermal gradient exists between junctions A and B (T1 and T2), an open circuit voltage of V is generated among C and D. the value of this voltage is proportional to the temperature difference and is identified by:

$$V = \alpha(T_2 - T_1) \tag{1-1}$$

where the α is the Seebeck coefficient usually measured in $\mu V/K$ and indicates the amount of generated voltage by a specific thermoelectric material per unit temperature difference [3].
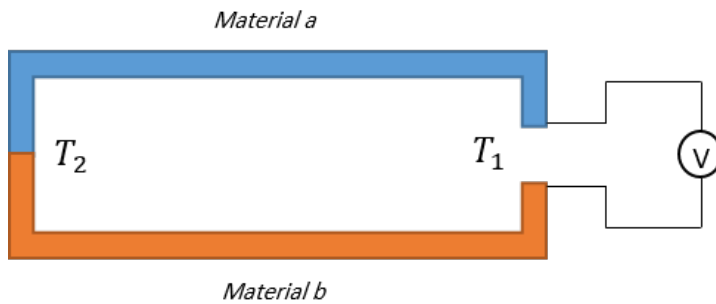
Fig. 1.2: A typical thermocouple consisting of two dissimilar conductors.

1.2.2 PELTIER EFFECT

The Peltier effect can be defined as the reverse of the Seebeck effect and was found in 1834 by Charles Athanase Peltier. Considering the circuit in figure 1.2, by imposing a voltage between points C and D and a current (I) passes through the circuit, a temperature gradient is generated at the two dissimilar conductors' junctions [3]. When the direction of this current is reversed, the hot and cold junction can be switched. The Peltier coefficient determines the relationship of this cooling/heating rate (q) and electrical current (I), and the unit is W/A.

$$\pi = \frac{q}{I} \tag{1-2}$$

1.2.3 THOMSON EFFECT

Thomson effect was introduced by William Thomson (later known as Lord Kelvin) in 1851[3]. Thomson recognized that if a temperature gradient happens inside a conductor, heat can be absorbed or lost by the conductor. This heat loss or absorption is changed with the electrical current's direction and is happened as a separate phenomenon from Peltier heating or cooling. The equation (1− 3) elaborates the amount of this heat loss and absorption corresponds to the temperature difference and electrical current:

$$q = \beta I \Delta T \qquad\qquad (1-3)$$

where β indicates the Thomson coefficient and has a similar unit with the Seebeck coefficient (V/K). In most research, the Thomson effect has not been considered in the thermoelectric model simulation since its amount is negligible compared with the Peltier effect.

1.2.4 FIGURE OF MERIT

The dimensionless figure of merit (zT) provides a metric to evaluate the thermoelectric functionality of a material [3]:

$$zT = \frac{\alpha^2}{\rho\kappa}T = \frac{\alpha^2\sigma}{\kappa}T \qquad\qquad (1-4)$$

This dimensionless metric is determined by the amount of the material thermal conductivity k, Seebeck coefficient α, temperature T, and electrical conductivity σ. Based on the equation (1 − 4), it is concluded that the amount of thermal conductivity and electrical resistivity (ρ) should be minimized for maximizing the figure of merit. This has been the focus of the thermoelectric research community to achieve higher values of zT. However, the main challenge in this way is the interdependency of the parameters which define the figure of merit. For example, most of the material is almost a case that increasing electrical resistivity happens simultaneously with increasing the material thermal conductivity. The typical value for the most high-performance thermoelectric material is around 1. However, some research groups claim to archives maximum values of 2.2 [4].

1.3 APPLICATIONS OF THERMOELECTRIC GENERATORS

There are many features associated with thermoelectric devices, making them interesting to be utilized for a vast area of applications. These devices' solid-state nature is a great advantage compared with other alternatives containing rotary equipment for both power generation and heat pumping. This means that they can operate without moving parts, with a high level of reliability, and almost maintenance-free during their long operating life.

1. **Space**, because of this reliability and long lifetime, thermoelectric generators have been used in many deepspace applications to power uncrewed spacecraft and independently from the sun radiation.
2. **Waste heat recovery**, thermoelectric generators are implemented for waste heat recovery over a wide range of temperatures (room temperature up to 1000 °C), based on the applied thermoelectric material. Automobile [3], [4], and marine exhaust [5], [6], industrial stacks [7], and exhausts [8] are examples of great opportunities to recover significant amounts of abandoned waste heats.
3. **Off-grid**, thermoelectric generators can also be used as an off-grid electricity source, especially in some developing countries where they do not have access to a reliable power grid or under an emergency condition. For example, they can be integrated into a thermoelectric stove to generate electricity by burning fuel directly [9]–[14].
4. **Sensors,** TEGs can generate power in the range of hundreds of microwatts to a few milliwatts in many situations, which makes them quite an interesting method for powering the low power devices. An example network of sensors can be integrated with a TEG and operate without any battery [15]–[18]. This is important, especially in the case of the sensors with a high degree of reliability like biomedical sensors [19]–[22] or sensors with no easy accessibility for replacing the battery, like condition monitoring sensors on top of an industrial riser [7].
5. **Solar**, is an alternative to the conventional photovoltaic generators, TEGs can convert solar energy to electricity by absorbing the sun's heat [5]. It is also possible to increase the overall efficiency by integrating the photovoltaic and thermoelectric generators into a single device [6].

1.4 FLEXIBLE THERMOELECTRIC DEVICES

Commercial TEGs typically are fabricated on rigid ceramic substrates and in small sizes. As a result, it is difficult to implement these inflexible devices for many real-world applications that contain surfaces with arbitrary shapes. For example, in powering a wearable device, the TEG should be attached to the human body, which has typically curved surfaces in most parts. A flexible TEG (Figure 1.3) can conform easily to the human body surface and decrease thermal loss [23]. It is also important to consider user convenience, which can be obtained easier by applying a flexible device instead of a rigid one [22]. Besides, there are heated curved surfaces in many industrial applications where the TEGs should be attached on. For example, the outer surface of a heated pipe (Figure 1.5) can be used as the installation surface of a TEG to power a condition monitoring sensor. Similar to the wearable cases, having a flexible TEG brings stronger thermal contacts and less thermal loss [7].
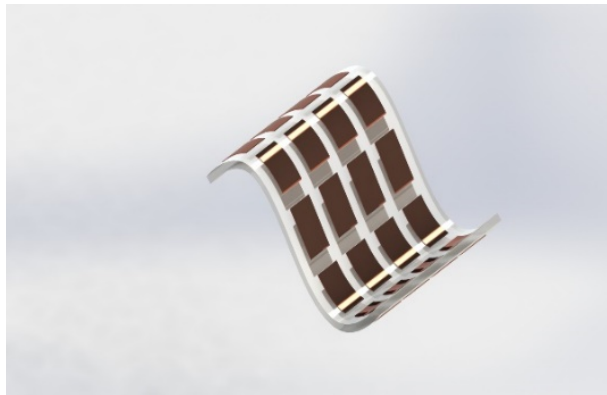
Fig. 1.3: Schematic of a flexible thermoelectric generator.

1.4.1 THERMOELECTRIC DEVICE MANUFACTURING

Commercial thermoelectric devices usually follow the manufacturing steps in Figure 1.4 [24]. It starts with thermoelectric powder sintering and alloying. The thermoelectric powder is then converted to cylindrical ingots through techniques like hot pressing or spark plasma sintering. The cylindrical ingots are cut in the desired thickness and being metalized afterward. The metalized pieces are cut into small pellets, mostly in a square or rectangular

shape. The cubic pellets are then placed manually or by a pick and place machine and bonded on rigid ceramic substrates by soldering or other alternative bonding methods. This approach has many disadvantages, like a high volume of material loss during the dicing process and thermoelectric pellet geometry limitations. Besides, it is vastly utilized to fabricate rigid and small thermoelectric devices. As a result, it is crucial to find novel manufacturing methods to decrease the overall thermoelectric system cost and manufacturing time that can also be utilized for flexible thermoelectric generators fabrication. For example, additive manufacturing approaches can bring many advantages in terms of raw material usage and arbitrary geometry formation [8].
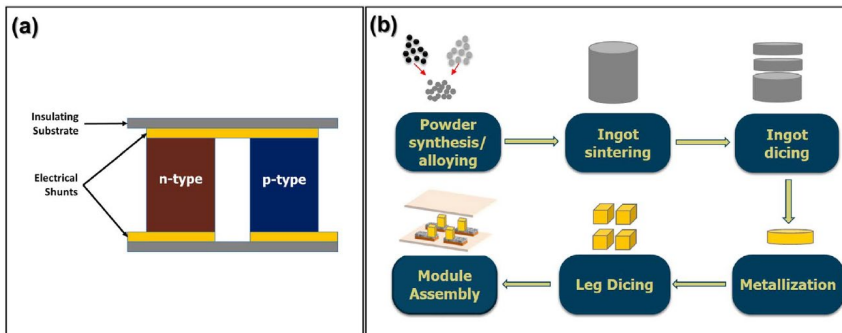
Fig. 1.4: Schematic of a flexible thermoelectric generator [8].

1.4.2 FLEXIBLE THERMOELECTRIC DEVICE MANUFACTURING

It has been two different approaches in order to fabricate flexible thermoelectric devices in the past. Some researchers have tried to obtain flexibility by introducing innovative design and using commercial solid thermoelectric materials such as rigid bismuth telluride pellets [7], [9]–[11]. In most of these cases, a flexible polymeric substrate is usually used in order to provide the required flexibility (Figure 1.5). The main advantage of these types of flexible modules is the comparable thermoelectric functionality to commercial thermoelectric devices. This is because of using the same bulk material applied in commercial modules that normally have the best available thermoelectric efficiency. On the other hand, the thermoelectric material itself is not flexible, and this rigidity makes it hard to achieve a fully flexible thermoelectric device.
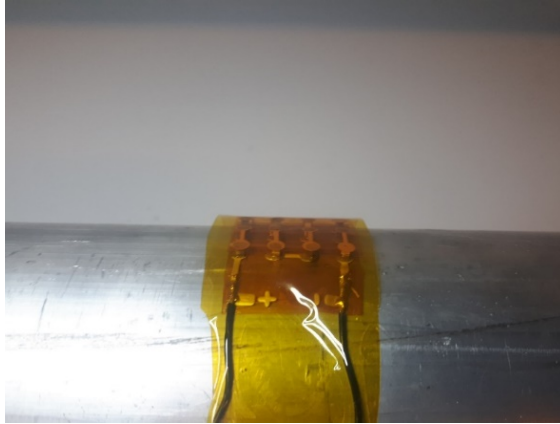
Fig. 1.5: Flexible TEG mounted on a pipe surface [8].

In the second direction, many attempts have been focused on providing flexible thermoelectric materials [12]. Polymer-based thermoelectric materials have been introduced as the best candidate in this regard [13], [14]. They are flexible, inexpensive, lightweight, and solution-processable. They have reasonably low thermal conductivity due to their highly disordered structure, which makes them appropriate for thermoelectric applications. But the main drawbacks are their very low Seebeck coefficient compared to their inorganic counterparts [12]. There have also been efforts to provide flexible and printable paste-like inorganic thermoelectric materials to print on a flexible substrate [15]–[17]. The power factors are still smaller by 3-4, compared with bulk inorganic material but even significantly larger than polymer-based thermoelectric material [15]. Despite these printable material's thermoelectric functionality, they can provide excellent opportunities for mass production of flexible thermoelectric devices by utilizing well-established approaches such as screen printing for high throughput roll-to-roll manufacturing (Figure 1.6) [18], [19]. Inkjet printing is also an interesting choice to dispense the thermoelectric ink on desired spots which can be controlled digitally [20]. It can minimize material loss and also the need for human labor.
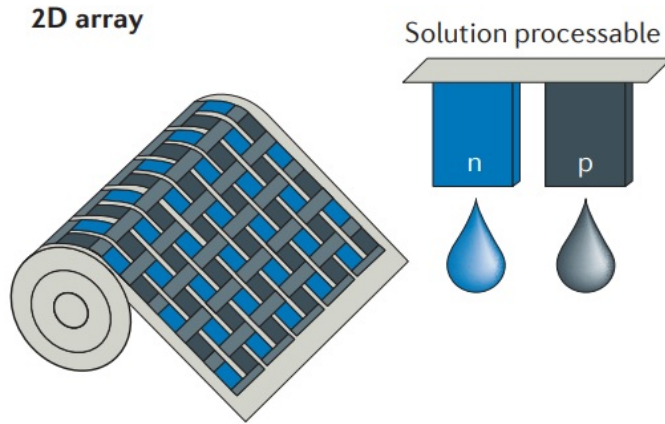
Fig. 1.6:   Roll-to-roll printing of thermoelectric materials [19].

The printable thermoelectric material can be formed into a device by two various configurations, vertical and lateral design (Figure 1.7 (a)). The first configuration is similar to the conventional thermoelectric devices, where the temperature difference happens across the thermoelectric material (Figure 1.7 (b)). In the second configuration, the temperature difference exists parallel to the substrate, as shown in Figure 1.7 (b).
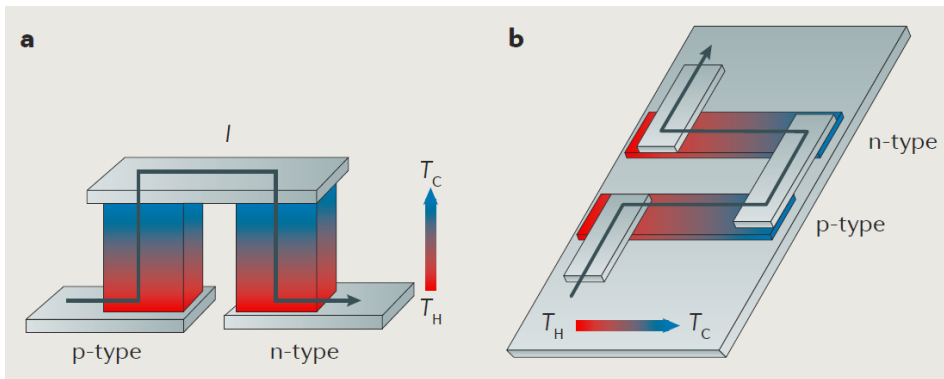
Fig. 1.7:   (a): TEG with vertical configuration, (b): TEG with lateral configuration [19].

Most of the printed devices have been based on the second configuration due to the fabrication simplicity and the in-plane direction of the carrier transport in solution-processed material [21]. Nevertheless, there is also a drawback to implementing this design for most of the real-world applications since the temperature gradient usually happens in the cross-directional rather than in-plane direction. One solution for this issue could be folding the flexible substrate to achieve the desired temperature difference across the device while maintaining its in-plane structure (Figure 1.7 (a,b)).
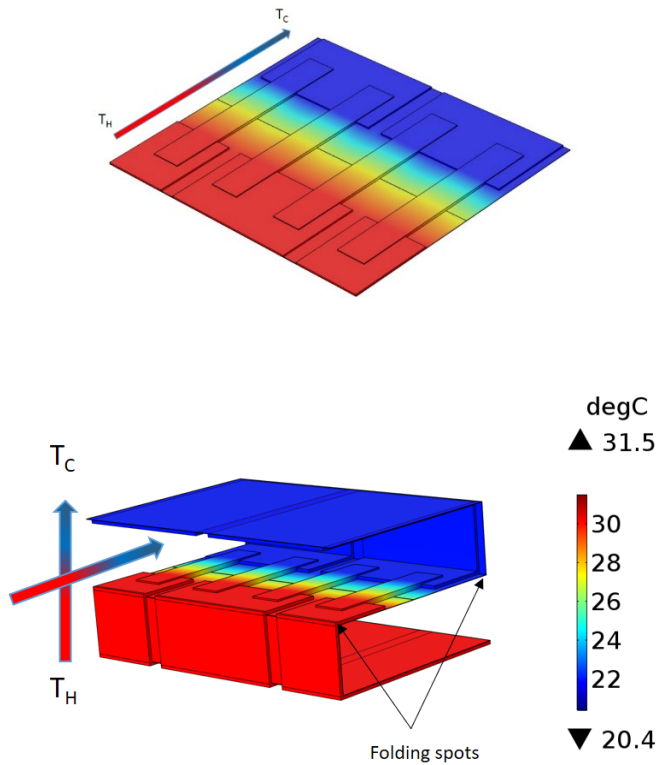
Fig. 1.8:   (a): In-plane heat flux for a planar TEG, (b): making a heat-conducting path by folding the flexible substrate [22].

There have also been much research works trying to deposit pure inorganic thin-film TE material in micrometer thickness to prove the feasibility of the vacuum deposition techniques for flexible thermoelectric modules fabrication [23]–[26].

1.5 THESIS OBJECTIVES

The general objective of this Ph.D. project is to develop novel manufacturing methods for high-throughput fabrication of flexible thermoelectric devices. In this regard, the following specific objectives are established:

1. planar flexible thermoelectric generator:
   a. Review of the different fabrication methods for adding thermoelectric materials on a substrate to form a planar thermoelectric device.
   b. Multiphysics modeling and optimization of a planar thermoelectric generator.
   c. Conceptualizing of flexible thermoelectric generators based on zinc-antimony thin-film.
   d. Thermoelectric characterization of the flexible zinc antimonide thin film-based device for low to medium temperature.

2. vertical flexible thermoelectric generators based on bulk bismuth telluride:
   a. Review of different manufacturing concepts to fabricate a flexible TEG based on bulk bismuth telluride material.
   b. Investigating various bonding methods to assemble the bismuth telluride pellets on a flexible polymeric substrate.
   c. Design and fabricate flexible thermoelectric generators based on bulk bismuth telluride on a flexible substrate.
   d. Thermoelectric functional characterization and flexibility tests for a flexible thermoelectric generator.
   e. Developing thermoelectric generators based on bulk bismuth telluride and for the temperature ranges over 200 °C.

1.6 THESIS OUTLINES

The dissertation consists of two main sections. In the first part, a summary report based on the published and submitted papers is presented. The second part of the thesis includes the Papers A-C that are already published or submitted for publication. The outcomes of this study are presented in six chapters. A summary of the content of each chapter in the first part of the thesis is given as follows:

Chapter 1: shortly elaborates on the fundamental of thermoelectricity and applications of thermoelectric generators. In continue, the manufacturing method for conventional thermoelectric generators is introduced. The importance of flexibility is discussed, and the advantage of having this feature for thermoelectric generators are presented through various application examples. The feasibility of different solutions to achieve flexibility for TEGs is shown based on different manufacturing concepts and materials.

Chapter 2: This chapter contains a detailed literature review based on thermoelectric devices' various fabrication methods. It starts with introducing various possible printing methods, continues with thin-film based thermoelectric devices, and ends up with flexible thermoelectric generators fabricated with bulk material.

Chapter 3: In the first section, a brief review of the possible printing method for planar thermoelectric devices is discussed. Design optimization for planar devices based on multiphysics modeling with a commercial software package is presented.

Chapter 4: This chapter presents a sputtering deposition method for developing thin-film based flexible thermoelectric devices. In continue, two design concepts are used for flexible module prototyping and thermoelectric characterization.

Chapter 5: In the beginning, a manufacturing platform based on flexible hybrid electronics (FHE) is elaborated. In continue, based on the proposed concept, a prototyping step is presented. At the same time, using nano-silver bonding as an alternative bonding method is justified for the bismuth telluride thermoelectric generators. Finally, thermoelectric characterization and flexibility tests are introduced to prove the functionality of the prototypes**.**

Chapter 6: This chapter summarizes this Ph.D. thesis and provides a road map for future works in the high throughput manufacturing of flexible thermoelectric generators.

CHAPTER 2. LITERATURE REVIEW AND STATE OF THE ART

A literature review on current research done in flexible thermoelectric generators (FTEGs) is presented in this chapter. It is categorized into three sections based on the nature of fabrication methods and the research conducted in this thesis.

2.1 PRINTED FLEXIBLE THERMOELECTRIC GENERATORS

2.1.1 SCREEN PRINTED THERMOELECTRIC GENERATORS

Screen printing is an already well-established technique to fabricate various electronic devices. During this process, a viscous ink is compressed through a pre-patterned stencil by using a squeegee. The viscosity of the ink and resolution of the stencil determines the aspect ratio and thickness of the final pattern. For example, it is possible to achieve a 100 μm thick layer with a 100 μm accuracy by utilizing a 50-pascal viscous ink [27]. This printing method's main advantage is its adjustability for high throughput manufacturing concepts like roll-to-roll printing (R2R), which enables high volume production of large-area flexible thermoelectric generators. It is also worth mentioning that screen printing has been the most popular method to fabricate printed thermoelectric devices. With both organic and inorganic material.

J. Weber et al. [28] tried to develop a printable thermoelectric paste of p-type Sb and n-type $Bi_{0.85}Sb_{0.15}$. They used various binders ethylene glycol, 2-component epoxy glue, and PMMA to form the final paste and to print on a Kapton tape. They have reported a power factor of 90 μW K^{-2} m^{-1} for their coil up flexible device without mentioning the curing condition. C. NAVONE et al. [16] developed screen printable thermoelectric ink based on (Bi, Sb)$_2$(Te, Se)$_3$ to be printed with the optimum thickness of 100 μm on a flexible polymeric substrate. Their paste could be cured at low temperature and claimed to have a high Seebeck coefficient value (90 μVK^{-1} to 160 μVK). They utilized a laser annealing process to enhance the power factor and obtained 0.06 μW K^{-2} cm^{-1}. Ju Hyung We et al. [29] proposed an annealing process to improve the functionality of the printable thermoelectric material. They suggested to heat the thermoelectric printed thick film to 500 °C for 15 min and claimed to achieve a power factor of 2.1 mW/m K^2 and thermal conductivity of 1.0 W/m K. The ZT value is 0.61at

room temperature. They also separately investigated the effect of annealing time on power factor and thermal conductivity and showed that the power factor is quite sensitive to the change in annealing time, and thermal conductivity is almost independent. Sun Jin Kim et al. [30] introduced a free-standing concept with no top and bottom substrate. It is possible to obtain a higher temperature range of annealing temperatures (530°C) due to the substrate-less configuration in their proposed concept. As a result, they reported large power factors of 1066 μW m^{-1} K^{-2} for n-type and 1166 μW m^{-1} K^{-2} for p-type material. They also screen printed the TE material into a glass fabric structure, which led to an acceptable degree of flexibility for their TEG. Z. Cao et al.[30] used the Cold isostatic pressing (CIP) technique in order to decrease the amount of electrical resistivity of the printed thermoelectric material. They altered the applied pressure and monitored the change of the Seebeck coefficient and the resistivity. They claimed to decrease the electrical resistivity form the 2.0×10^{-2} Ω·cm reported in the literature to 5.01×10^{-3} Ω·cm by this approach. Tony Varghese et al. [31] applied a microwave-stimulated wet-chemical method to synthesized nanocrystal ink to be screen printed on a flexible polyimide substrate. The printed film was treated by cold compaction and sintering to reach superior thermoelectric functionality. They indicated a pick value of 0.43 for the n-type figure of merit and a high power density of 4.1 mW/cm^2 for the thermal gradient of 60 °C. They also proposed to add thioglycolic acid (TGA) as a surface capping agent, which can prevent the oxidation of nanocrystal ink oxidation. Sunmi Shin et al. [32] used methylcellulose as the binder additive, which could provide proper viscosity for printing at low concentrations (0.45–0.60 wt.%). This could be beneficial since the binder agent typically decreases the thermoelectric performance of the printed film due to the negative impact on the electrical transport of the thermoelectric layers. They found nanoscale defects inside the n-type material after eliminating the binder by heat and reported a decrease in lattice thermal conductivity as a result of that. Their printed film showed high room-temperature zT values of 0.65 and 0.81 for p-type and n-type, respectively. Hyeongdo Choi et al. [32] tried to improve the performance of the printed TEGs differently. They focused on enhancing the function of the electrodes by introducing high-density silver electrodes. This was achieved by developing a UV curable silver paste, which showed fewer numbers of pores inside the electrode structure comparing to the other reported electrode materials. Minimizing the number of pores resulted in decreasing the penetration of soldering material into the electrode section and enhancing the electrodes' performance. Pin-Shiuan Chang et al. [33] fabricated a planar TEG by screen printing and pressure sintering. They also proposed a directional heat design to optimize the thermal gradient of their planar device. The device managed to generate 50 μW at a temperature difference of 54.9 °C. They sputtered Ni layer to act as the electrodes and then heated up the device up to 345°C under a pressure of 25 MPa. Their device also showed proper functionality after imposing a 1000 cycles bending test. Tony Varghese et al. [34] developed a new method to enhance the printable

thermoelectric paste's performance by adding a tellurium-based nano-solder agent. This can make a stronger bond between the BiSbTe particles during the sintering step, ultimately improving charge carrier mobility. They reported a power factor of 3 mW m^{-1} K^{-2} and ZT about 1, significantly higher than any previously reported performances for printable TE material. Their approach can convert thermoelectric nanoparticle into high-performance thermoelectric film and be tailored for the mass-production of printed flexible TEG.

In addition to developing bismuth telluride-based printable TE material, some researchers have been focused on printing polymer-based TE material. In comparison with inorganic material, they are more flexible, cost-effective, and scalable for high throughput printing, but they still have low thermoelectric efficiency.

Qingshuo Wei et al. [35] screen printed organic thermoelectric material based on conducting polymer poly(3,4-ethylenedioxythiophene):poly(styrenesulfonate), PEDOT:PSS, on a paper substrate. They sandwiched numbers of these substrates, containing the arrays of printed PEDOT:PSS films to form the final device and managed to obtain 50 mW with an open circuit voltage higher than 40 mV at a temperature difference of 100 °C. Roar R. Søndergaard et al. [18] utilized R2R printing to fabricate a flexible TEG comprising 18000 printed thermoelectric elements in a planar configuration. The printed PEDOT:PSS thermoelectric films were connected by silver electrodes to form the final device large area structure. They proposed a design that can fabricate a uni-leg (only p-type) device due to the lack of proper n-type polymer-based thermoelectric material. Ju Hyung We et al. [36] formulated a hybrid organic and inorganic composite for screen printing. They introduced the poly(3,4-ethylenedioxythiophene):poly(styrenesulfonate), PEDOT:PSS into the printed inorganic film's micropores to increase the overall flexibility. They also claimed that this method increased both electrical and thermal conductivity. They managed to generate a power of 1.2 mW cm^{-2} at a 50 K temperature difference and prove their device's functionality under bending condition.

2.1.2 INKJET PRINTED THERMOELECTRIC GENERATORS

Inkjet printing has been the focus of many attempts to fabricate electronic components. In this method, the drops of functional inks are deposited on desired patterns through a digitally controlled piezoelectric dispenser. There have been many efforts to develop printable thermoelectric ink for this technique due to the many advantages such as scalability, high precision, and minimal material waste. Ziyang Lu et al.[37] during one of the earliest work, developed p-type $Sb_{1.5}Bi_{0.5}Te_3$ nanoparticles and n-type $Bi_2Te_{2.7}Se_{0.3}$ inks. Aqueous solutions

of the nanoparticles were prepared by using a commercial stabilizer. The resulted thermoelectric arrays were connected by printed silver electrodes to form the device's final planar configuration. They reported a power factor of 77 μW m^{-1} K^{-2} for n-type and 183 μW m^{-1} K^{-2} for p-type materials. The main drawback of their approach is the necessity of applying a high annealing temperature, which can lead to damaging the flexible substrate. Chen et al. [38] develop nanowires based thermoelectric ink only for n-type material and both for n- and p-type material during a complementary effort [39]. They used liquid metal eutectic gallium–indium (EGaIn) as the interconnects that could be deposited to form a fully printed device. Similar to the previous works, their printable TE ink requires a high temperature for annealing. Developing a conducting polymer-based printable ink could be an alternative to the inorganic inks, which can also solve applying high annealing temperatures. Bubnova et al. [13] inkjet printed a combination of a solution of EDOT monomer and oxidant (Fe(Tos)$_3$) as the PEDOT:Tos is not soluble. They used Ag electrodes, which are pre-patterned on a flexible substrate. The final device showed a higher level of power factor compared with the previous inorganic based printable material. There also have been efforts to develop hybrid organic inks bay adding inorganic nanoparticles. Besganz et al. [40] change the altered concentration of PEDOT:PSS-ink by the inclusion of mixed ZnO nanoparticle. It was shown that there is a trade-off between the amount of ZnO nanoparticles and TE ink functionality, and the optimum performance was reached by mixing 20% ZnO. They heated up the printed arrays up to 150 °C, which does not seem sufficient considering the existence of ZnO nanoparticles. Ferhat et al. [41], for the first time, tried to develop n-type printable material by introducing a composite of PEDOT and V$_2$O$_5$, 5H$_2$O gel. Triton X-100 tuned the viscosity of the ink as the Detergent additives. The fully printed device on a paper substrate consisted of PEDOT:PSS, (PEDOT)$_x$V$_2$O$_5$ and silver ink as the p&n type material and electrodes and was cured at 100 °C. their proposed n-type material showed a power factor of two orders of magnitude smaller than its inorganic counterparts. The carbon-based inks also have been studied as the printable TE ink. Park et al. [42] applied carbon nanotube CNT as both p-type and n-type materials and PAA and PEI as the dopant agents. They controlled the carrier concentration with these dopant agents and reported a power factor of 129 and 135 for p-type and n-type, respectively. The obtained results were quite comparable with other alternative printable materials and could open the door to the vast development of CNT based printed TEGs.

2.1.3 DISPENSER PRINTED THERMOELECTRIC GENERATORS

It is possible to fabricate a thermoelectric device by additively dispensing the thermoelectric material on a flexible substrate through a dispenser nozzle. The material exits the nozzle head in the form of a continuous filament and by means of pneumatic or mechanical pressure. Through adjusting the ink viscosity, nozzle feed rate speed, and the nozzle gap between the substrate, printing entities as small as 250 nm are achievable [43]. It is also possible to deposit material in the form of a thick film, even with a thickness of 200 μm [15]. There have been more advanced dispensing techniques recently to deposit materials faster and with higher resolution. For example, the electrohydrodynamic (EHD) nozzles deposit the droplets of ink by applying a controlled electric field. In this way, a precise resolution (100 nm) is obtainable by applying high-frequency pulses for the EHD system [44]. This method provides maskless patterning of functional materials on a targeted substrate, which minimizes the amount of wasted material, but providing proper printable material is also a considerable barrier to fully used this method as a replacement for other well-established printing techniques. The earliest works for dispenser printing started by developing printable paste based on n-type Bi_2Te_3 and p-type Sb_2Te_3 [15], [45]. They used a polymer binder to form the final paste and cured the paste at a relatively low temperature of 250 °C due to the Kapton substrate's temperature sensitivity. Because of the polymer binder's inclusion, the thermoelectric paste had a poor thermoelectric functionality compared to the bulk materials (almost two orders of magnitude).

Consequently, they tried to decrease this gap during some complementary attempts by utilizing methods such as mechanical alloying and Se and Te doping [46], [47]. Wu et al. c [48] integrated dispenser printing with selective laser melting (SLM) to maximize the printed material's thermoelectric efficiency. But due to the system complexity of the SLM method, the proposed method is not applicable widely. Jo et al. [49] used a disperser printer to fill up cavities inside a PDMS body to form a cross-sectional device. They reported 2.1 μW power at a 19 K temperature difference for their 50 × 50 mm device.

2.1.4 AEROSOL JET AND SPRAY PRINTING

In aerosol jet printing, the ink particles (20 nm to 5 μm) are jetted through an inert gas or compressed airflow on a targeted substrate. The ink particles are aerosolized by an atomizer and can be deposited with a larger gap between the nozzle and the substrate. This enables printing on substrates containing curved or rough surfaces and with a resolution even higher than inkjet printing. But the quality of the edge sharpness is not high compared to inkjet

printing, and the adhesion of the bonding layers also is affected by partial crystallization. Canlin et al. [50] developed an ink containing high-S Sb$_2$Te$_3$ nanoflakes, high-conductive multi-walled carbon nanotubes (MWCNTs), and PEDOT:PSS and deposited by aerosol jet printing on a flexible substrate. They reported power factors of ~41 µW m^{-1} K^{-2} by adjusting the best combination of the substances and surface treatment. Mortaza et al. [51] introduced photonic sintering to significantly increase the electrical conductivity of the printed film to 2.7×10^4 S m^{-1} and consequently boost the power factor to the substantial amount of 730 µW m^{-1} K^{-2} . their ink was based on Bi$_2$Te$_{2.7}$Se$_{0.3}$ nanoplate. Cheon et al. [52] fabricated a flexible device by spray-painting a nanocomposite ink, including CNT and P3HT, on a Kapton substrate. Their device had only p-type thermoelectric legs and showed a power factor of 325 ± 101 µW m^{-1} K^{-2}.

2.2 THIN-FILM FLEXIBLE THERMOELECTRIC GENERATORS

The low conversion efficiency and high cost have been major obstacles to the wide commercialization of bulk thermoelectric material. One strategy for handling these issues could be fabricating thin-film thermoelectric (TFT) devices. TFTs have smaller lattice thermal conductivity compared to bulk materials due to the proper phono scattering [57]. It has been found in many studies that the superior thermoelectric functionality of TFTs is related to the quantum well effect and superlattice structure [58]. In continue, most common manufacturing methods for deposition of inorganic thin-film material are explained.

2.2.1 SPUTTERING DEPOSITION METHOD

The thin-film is made by depositing layers of a target material on a substrate during the sputtering process. High-energy particles hit the surface of the target material to remove the atoms in a vacuum. Sputtering generally classified into two methods, direct-current (DC) sputtering and radio-frequency (RF) sputtering. The difference between the two approaches is related to the power source they implemented for creating the plasma inside the vacuum chamber [53]. Byeong Geun Kim et al. [54] investigated the effect of the different substrates on the quality of the deposited film. They used three substrates, Si wafer, glass, and polyimide for deposition of Cu-doped Bi$_2$Te$_3$ by magnetron sputtering. They detected thermal stress during the deposition process due to the difference between the materials' coefficient of thermal expansion. They concluded that the highest thermal stress occurs when the Kapton is applied as the substrate. Zhaokun Cai et al. [55] fabricated thin films of N-type Bi$_2$Te$_3$ and p-type Sb$_2$Te$_3$ by RF and DC co-sputtering. They reported the Seebeck coefficient of -122 µVK^{-1} and 108 µVK^{-1} and power factor of 0.82×10^{-3} Wm^{-1}K^{-2} and 1.60×10^{-3} Wm^{-1}K^{-2} for the

n- and p-type, respectively. They used a glass substrate with a multi-target sputtering method. Coppers electrode was also deposited by DC and with a thickness of 1μm. In an attempt to decrease thermal stress's negative effect, Deyue Kong et al. [56] encapsulated their thin film by a layer of poly (dimethylsiloxane). They also claimed to obtain a 21.7 $\mu W/cm^1K^2$ power factor for their Bi_2Te_3 film by controlling the sputtering pressure. Their device also showed only a 5% deviation in its functionality after passing a 2000 cyclic bending test. They also tested the device on the human body condition and reported an open circuit voltage of 12.99 mV. S. Kianwimol et al. [57]specifically analyzed the sputtering power's effect in the thin-film deposition of Bi_2Te_3 on a Kapton substrate. They showed the Te content's dependency and grain size to the sputtering power while using the DC magnetron sputtering. Based on their results, the Te content shows a reduction trend by increasing the sputtering power. They reported the pick power factor of 5.4×10^{-3} W/m K^2 at a temperature of 300 °C. Fan et al. [58] utilized a DC sputtering for Bi and Sb and RF sputtering for Te target to fabricate n-type Bi_2Te_3 and p-type Sb_2Te_3 films. They proposed an inplane device configuration and fabricated a device with 20 p-n thermoelectric couples. They deposited copper electrodes on a ceramic substrate and then used silver paste to bond the film on the substrate. Their device was able to generate the pick power of 19.13 μW at the 85K temperature difference. The same research group utilized DC magnetron sputtering to fabricate p-type Zn-Sb based thin film and n-type ZnO:Al thin film [59]. They mentioned that due to the lower cost of zinc antimonide based material compared to BiTe-based thin films, their device could open the door for more applications of thin-film generators. They also used a flexible substrate for deposition, which is more suitable for high volume production. They claimed maximum power of 246.3 μW when the temperature difference is 180 K.

2.2.2 ELECTRODEPOSITION METHODS

A thin film is formed by the electrochemical reduction of metal ions in an electrolyte during the Electrodeposition technique. The electrodeposition is categorized into two parts: electrolytic and non-electrolytic platings. Typically, a standard three-electrode cell is applied to contain working, reference, and counter electrodes Compared to the other dry methods. This approach is cost-effective and can be conducted at a lower range of temperatures (80 ℃). It is also quite a fast technique, that can fabricate thick film materials with a high deposition rate. The main issue with the electrodeposition of TE thin films is the limitation of this deposition approach only on conductive surfaces.

Snyder et al. [60] fabricated microelectromechanical (MEMS) like thermoelectric devices containing 126 n-type and p-type (Bi, Sb)$_2$Te$_3$ thermoelectric legs. They used a 400-μm-thick

oxidized silicon substrate and selected a photoresist mold to deposition the thermoelectric legs. They managed to fabricate thermoelectric legs as small as 20 μm in height and 60 μm in diameter. Liu et al. [61] offered a multi-channel configuration to fabricated a microscale thermoelectric generator. They first formed these microchannels inside a glass mold, and then introduced a technique to fill these cavities by electrodeposition. They proposed to implement a reverse pulsed electrodeposition method in order to avoid any gaps in the deposited material. They claimed that their deposited Bi_2Te_3 had a comparable chemical composition to the conventional Bi_2Te_3 material. Matsuoka et al. [62] analyzed the effect of Te content in the electrodeposition of Bi_2Te_3 thin-films. They showed the dependency of the Seebeck coefficient, electrical conductivity, and type of the thermoelectric material (p,n) to the amount of Te. They stated that this could be helpful as the type of thermoelectric material is simply determined by altering the quantity of Te. They applied a nickel plate to electrodeposit Bi/Te thin-films in a hydrochloric electrolyte. Multilayer n-type BieTe/BieSe thin-films were fabricated by Matsuoka et al. [63] with a dual-bath electrodeposition approach. The thickness of their films was kept at 1 μm while the number of the deposited layers was changed between 2 to 10. They reported the same Seebeck coefficient for the different number of layers and a greater electrical conductivity for the films with more number of layers. They mentioned that it could be related to increasing the electron mobility by reducing the thickness of the individual layer. They managed to generate the maximum power factor of 1.44 mW/(cm K^2) for the film with ten layers.Takemori et al. [23] considered the impact of thermal annealing and homogeneous electron beam (EB) irradiation in enhancing the electrodeposited BieTe based thin-films. They proved that the crystallographic characteristics could be boosted by thermal annealing, which eventually leads to an enhancement in thermoelectric functionality. They also showed the independency of the film properties from the EB irradiation treatment.Takashiri et al. [64] proposed to utilize a BiTe seed layer on a glass substrate in order to enhance of crystallinity of the films. This seed layer was first sputtered and followed by thermal annealing afterward. They claimed to increase the power factor of the as-grown films by a factor of eight only by implementing this seed layer and significantly increasing the amount of electrical conductivity. Yamaguchi et al. [24] studied the effect of altering the temperature and concentration of the electrolyte on the quality of the electrodeposited BiTe films. They reported a reduction in thermoelectric functionality by increasing the electrolyte temperature. It was mentioned that it is due to the formation of dendrite crystal structure in the films, which can negatively affect the surface morphology of the films. They also stated that the surface morphology of the deposited film is not dependent on the concentration of Bi Te contents in the electrolyte.Yamauchi et al. [65] offered a solution for the thermal conductivity measurement of the electrodeposited films. They implemented various acid solutions to improve the surface roughnes of the films and used 3ω approach for thermal conductivity measurement. They mentioned the ability of this measurement only for the films

deposited in nitric acid (HNO_3) solutions and reported a low thermal conductivity of 0.14 W/(m.K) for their film. They stated that the low amount of thermal conductivity is due to the amorphous structure of the films. Su et al. [66] developed a thermoelectric device containing micropillar thermoelectric legs which are electrodeposited into a microporous glass substrate. They used a three-step pulsed-voltage deposition method to fill the microcavities with a high deposition rate and quality. They also investigate the negative effect of over potential on the quality of the deoposited film. They stated that electrical conductivities, power factors, and carrier mobilities are reduced significantly by increasing the value of the over-potential. They reported 6.22 Ω for a single deposited micropillar with a dimension of 60 μm in diameter and 200 μm in height.

2.3 BULK-FLEXIBLE THERMOELECTRIC GENERATORS

There have been many attempts to fabricate a flexible TEG by using conventional bulk materials [9]–[11], [67]–[70]. The main reason to utilize these rigid materials is their far better thermoelectric efficiency compared to other organic and in-organic printable thermoelectric materials. Besides, depositing and printing thermoelectric materials in the form of thin films could not guaranty the required thermal gradients for power generation in most of the real-world applications. Nevertheless, to bring flexibility to the bulk-based TEG, special design and structure should be considered. Park et al. [68] designed and fabricated a mat-like fixture to hold the bulk thermoelectric pellets of BiTe. Flexible wires connected the thermoelectric legs, and the gap between them was filled by air. They tested the device for an on-body thermal comfort experience and managed to generate a 4 K temperature drop. They also used the device in on-body power generation mode and managed to achieve 88 μW, which is a considerable value for powering most of the wearable electronics. Eom et al. [69] introduced a modular configuration that could be wrapped around a curved surface like a human wrist. Their device was able to generate 80 μW while the user at rest. They also implemented a heatsink for their wearable device that helped to generate more power from the body. Flexible copper wires were used as the interconnects, which enable them to bend the device freely. Their device also showed a high thermal contact resistance level due to the large thickness of the copper interconnects. Park et al. [70] developed a flexible fixture for holding the rigid thermoelectric pellets. They used a flexible printed circuit board (FPCB) to connect these pellets after fixing them inside the flexible fixture. The flexible interconnects provided an acceptable degree of flexibility but poor electrical conductivity due to the low thickness. As a result, to consider both aspects, they attached two layers of copper electrodes with a thickness of 12 μm. The device was also examined in refrigeration mode by applying a portable battery and making a 4.4 K temperature difference on human skin. They also

reported a power density of 5.6 $\mu W.cm^{-2}$ for power generation mode from the human body. Kim et al. [71] fabricated a flexible device by bonding the thermoelectric legs to the flexible copper electrodes as a stand-alone configuration. They developed specific filler material with low thermal conductivity to cover the gaps between the thermoelectric legs as well as provide the necessary mechanical strength. Their device was examined based on the human body surface model containing a curved surface and heater to prove the functionality during a bending condition. They also provided the relationship between the geometry of the thermoelectric legs and the device fill factor to the amount of generated power in the case of the human body heat recovery. Wang et al. [22] utilized a modified flexible printed circuit board (FPCB) to bring more levels of flexibility to their thermoelectric device. They patterned the substrates with holes between the electrical pads and filled the device with PDMS for more mechanical stability. They fixed the lower substrate and used a fixture for thermoelectric legs positioning and solder bonding. The device was tested on a human wrist to evaluate the powering of a miniaturized accelerometer. They managed to achieve a 6.6 mV for a thermal gradient of 5.8 K, which is sufficient to power the accelerometer. Suarez et al. [72] applied eutectic gallium indium (EGaIn liquid metal) as the electrodes to connect thermoelectric pellets. The liquid interconnectors can easily tolerate the bending condition and show self-healing behavior when placed at a curved surface. Simultaneously, it is difficult to seal a device with liquid features, especially when it has to be bent or moved. The use of polymeric sealing material can also increase the thermal interface parasitics and consequently decrease the value of the generated power. The same team in a newly published work [73] developed a special polymer with high thermal conductivity, which can boost the function of the device by a factor of 1.7. They also added a copper heat spreader and claimed to increase the power 1.3 times. Their device was able to generate a maximum power of 30 $\mu W.cm^{-2}$ at an air velocity of 1.2 m/s. T. Sugahara et al. [74] investigated the fabrication process of flexible TEGs from a different perspective. They utilized semiconductor packaging technology containing high-speed pick and placing and bonding to justify the possibility of the approach for large scale manufacturing. They conducted a cyclic bending test and shear strength test to prove the reliability of the device under the bending conditions. Their device managed to generate the pick power of 158 $\mu W.cm^{-2}$, which is the highest among the works that have been reported for bulk flexible TEGs.

CHAPTER 3. FLEXIBLE PRINTED THERMOELECTRIC GENERATORS AND DESIGN OPTIMIZATION FOR WEARABLE APPLICATIONS

One of the barriers on the way of industry scale utilization of the thermoelectricity is the lack of cost-effective and high throughput manufacturing methods. As a result, many researchers have been focused on adopting well established printed technology to fabricate thermoelectric devices. Printing techniques are fast and cheap compared to other material deposition methods, which can additively deposit material on flexible substrates. But there are many challenges associated with adopting printing techniques for thermoelectric module fabrication, such as designing suitable printable thermoelectric material and obtaining the printed thermoelectric material's required resolution. Among the printing methods, screen printing is the most versatile and well-established technique that can easily be customized for high throughput manufacturing scenarios like roll to roll printing. In this section utilizing various printing methods for thermoelectric materials is discussed, and an approach for design optimization of the printed TEGs is introduced.

3.1 PRINTED THERMOELECTRIC GENERATORS DESIGN

There have been two main design configurations for the printed thermoelectric generators in past studies. In the first configuration, the heat flux direction is perpendicular to the substrates (Figure 1.7 (a)). This is the most commonly used configuration, typically applied in the manufacturing of commercially bulk thermoelectric devices. In order to print a thermoelectric device in the vertical configuration, a stack of printable thermoelectric material should be deposited on desired locations. This could be accomplished by means of a digitally controlled deposition technique such as dispenser printing, which is capable of 3D printing functional material. It is also possible to print a thick layer of thermoelectric material on a substrate by screen printing. The technique can deposit a layer with hundreds of microns in thickness,

which may be sufficient for device fabrication. Hence, the various aspect ratios for thermoelectric legs (height to width) could not be obtained by one-step printing. This issue can be handled by designing ink rheology properly and multi-layer printing. In the second configuration (Figure 1.7 (b)), the heat flux happens in the direction of the substrate plane. In terms of printing technology, this architecture has been vastly studied for many areas of application. The printing of functional materials in a planar configuration containing various conducting material interfaces is already a well-established area for the printing industry. The problem with the planar printing structure of thermoelectric materials is mostly related to the adhesin of the printed materials to the formerly printed layers as well as the flexible substrates. Besides, a sufficient temperature difference should be provided when a planar TEG is installed on a heated surface to harvest thermal energy. Since in most cases, the heat flux exists in the device cross-sectional direction, which should be guided properly in the case of the planar printed thermoelectric generators. For example, by considering the special heat-conducting path by folding the substrate (Figure 3.1) to maintain enough temperature difference on two sides of the thermoelectric legs despite the in-plane heat flux direction.
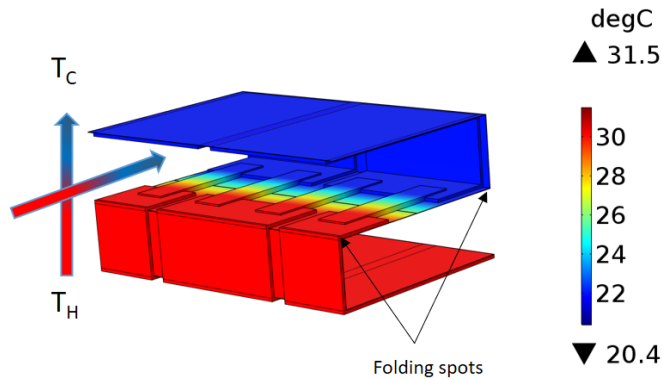
Fig. 3.1: Floding the substrate to create a heat-conducting path [22].

3.2 SCREEN PRINTED THERMOELECTRIC GENERATORS

Screen printing was initially applied to various printed electronics applications in large volumes. The technique also is utilized for fabricating different types of sensors and actuators. Typically, there are four steps during a screen printing process: printable paste formation, dispensing the paste in desired patterns, drying, and curing. Based on the required shape and resolution, a screen with a defined mesh size is fabricated initially. Normally it is possible to print the inks with a viscosity in 3000 to 25000 cP [71]. The deposition of printable paste is typically performed in 3 steps (Figure 3.2). In the beginning, the printable paste is placed on top of the screen and dispersed along the surface by a blade. Then the paste is pressed by a squeegee through the pre-patterned areas to form the desired geometries. The screen is detached from the printing substrate, and the printed patterns are formed. By printing multiple layers with the same pattern, the thickness of the printed features can be customized. During the multi-layer printing, each layer should be dried before printing the next layer to keep the material in place and form mechanical support for the next layer. The properties of the organic binder inside the printable paste define the required drying conditions. The resolution of 10 μm – 100 μm is achievable for a printed layer based on the paste properties. The printed patterns should be cured lastly to obtain the required adhesion to the substrate and targeted mechanical characteristics. The most critical parameters for successful printing are the squeegee feed rate, pressure, orientation, and gap distance.

Until now, there have been attempts to develop both organic and inorganic printable pastes for the screen printing process. There are many challenges on the way of realization of a practical printable thermoelectric material. For example, Satisfying both the thermoelectric functionality and printability could be quite problematic since the amount of thermoelectric functional feature inside the printable paste directly affects the printable paste's viscosity and rheology. The BiTe printable pastes mostly contain the thermoelectric material's powders and an epoxy binder (Figure 3.2 (a)). The viscosity of the ink is also set by adding a solvent. These BiTe based materials are normally cured at the temperature range between 250 °C to 350 °C and a drying holding time of 3 hours. A complementary step, such as hot pressing, could be added to the process boosting both the mechanical and thermoelectric properties of the final film.
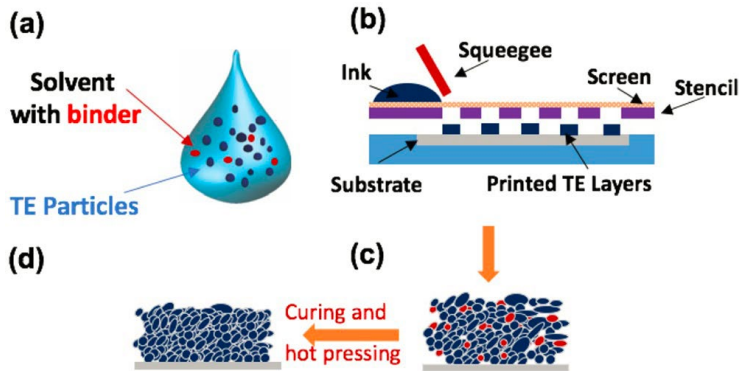
Fig. 3.2: Screen printing of bismuth telluride printable paste [72].

There are some issues with the inorganic based thermoelectric materials, such as the high cost, inflexibility, and toxicity. It is also worth mentioning that these materials require a high-temperature level for curing, which cannot be tolerated by most polymeric flexible substrates. Polymer-based materials are exciting alternatives to inorganic based material, which can solve most of the mentioned problems. They are flexible in nature, non-toxic, cheap, and easily customizable for high throughput manufacturing. However, despite the low thermal conductivity, they cannot compete with their inorganic counterparts in terms of power factor. Most of the works in this area focused on developing ink based on conducting polymers like PEDOT: PSS [14]. These materials' main advantage is the solution processability, making them quite attractive for large-volume fabrication such as roll to roll printing (Figure 3.3).
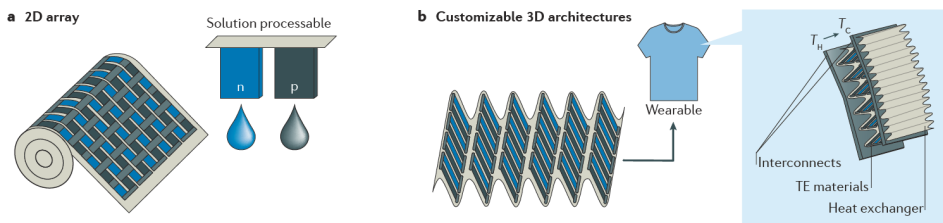

Fig. 3.3: Large area printing of organic-based printable thermoelectric materials in roll (a) and conjugated(b) form [19].

3.3 DISPENSER PRINTED THERMOELECTRIC GENERATORS

Dispenser printing is an approach for maskless deposition of functional materials with feature resolutions down to 250 nm. By this technique, a continuous filament of material in the form of a viscous ink is added by a pneumatic or mechanical dispenser onto a substrate Figure 3.4. Some parameters control the quality of the printed features, such as the nozzle gap with the substrate, dispenser head feed rate, and rheology of the printable material. It is also possible to deposit thick films with a thickness of 200 μm [15]. Conventional pneumatic dispensers could be replaced by state of the art electrohydrodynamic (EHD) dispenser valves in order to achieve even a higher level of printing precision (100 nm) and speed [44]. This maskless approach results in a significant amount of raw material consumption due to the possibility of printing materials on demand.

On the other hand, providing functional viscous thermoelectric ink is problematic. Such as the screen printable thermoelectric paste, the inclusion of the binder agent in the paste materials results in a considerable reduction of the thermoelectric function compared to the conventional bulk material. There are some ways to reduce this gap, such as mechanical alloying and doping, yet the gap is significant.
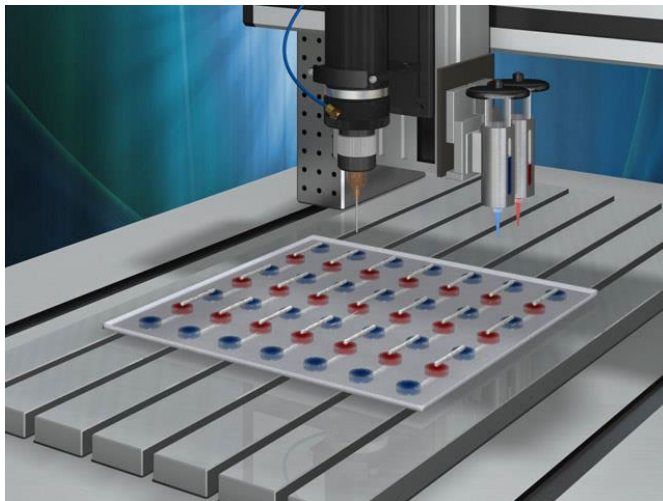
Fig. 3.4: Features of a dispensing system for thermoelectric material © Fraunhofer IWS Dresden.

3.4 DESIGN OPTIMIZATION OF A PLANAR PRINTED THERMOELECTRIC GENERATOR

As mentioned in section 3.1, the planar configuration has a great potential for high throughput manufacturing scenarios due to the simplicity of the printing traces of the functional materials with techniques such as screen printing. As a result, most of the flexible thermoelectric devices have been developed with an in-plane architecture (Figure 3.5) and a carrier transport path in a flexible substrate plane.
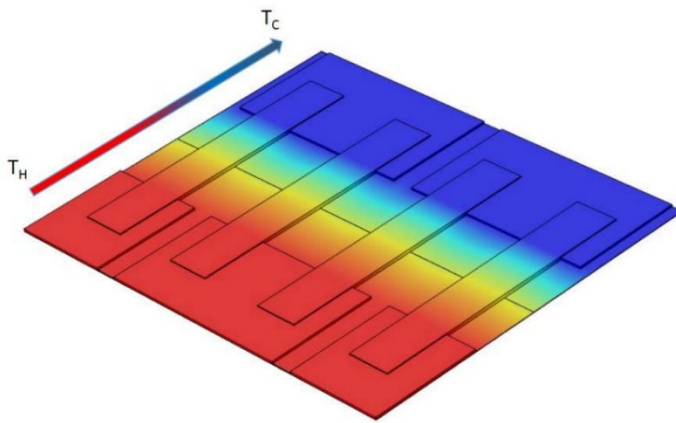
Fig. 3.5: Heat distribution for a planar printed TEG [22].

Despite the advantages of the planar configuration, it can not make a sufficient temperature difference across the device due to the thermoelectric materials' tiny thickness. This issue can be handled by introducing novel designs, such as providing a heat-conducting path for the printed TEG (Figure 3.6). In such a concept, the heat's overall direction is perpendicular to the device cross-section plane, while the heat flows in the printed thermoelectric material plane (Figure 3.6 (b)). The desired heat conduction path can be obtained by folding the flexible substrate in defined directions to form the final device structure. As shown in Figure 3.6 (b), temperature difference boosting can be substantial compared to the flat planar device with no heat-conducting path that can only hold a thermal gradient less than a degree of Celsius (Figure 3.6 (a)). This concept can be further customized for high throughput manufacturing like roll to roll in the form of the printing step and folding step.
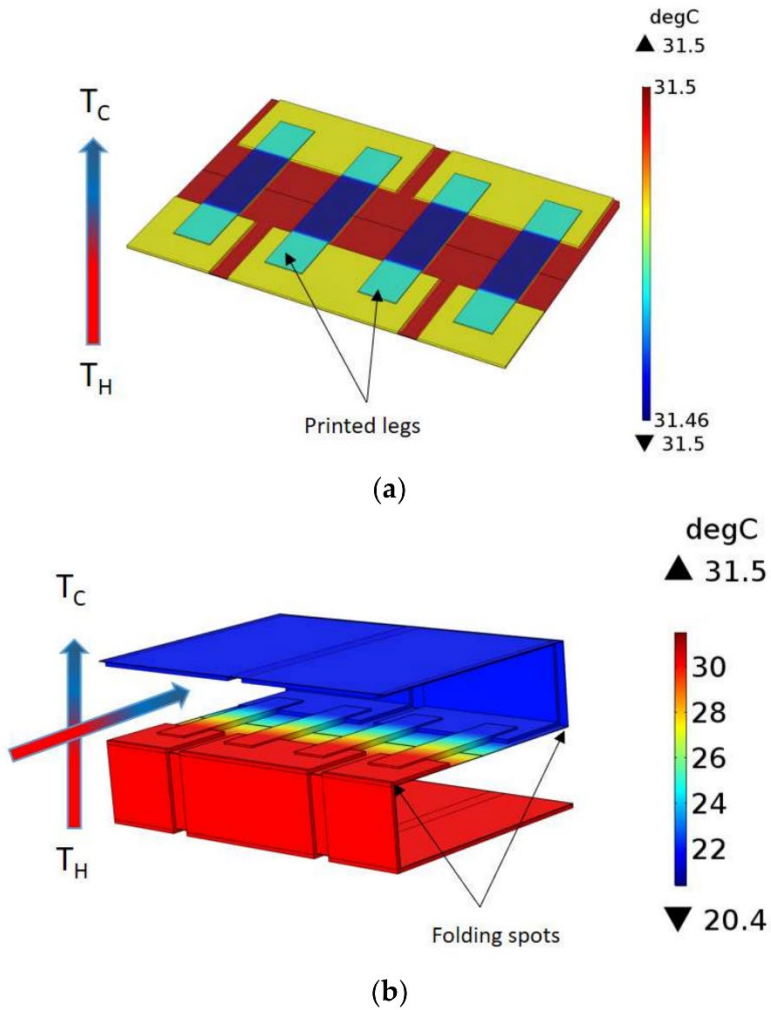
Fig. 3.6: Distribution of heat for a planar TEG: (a) without folding, (b) by folding, and making a heat-conducting path [22].

Multiphysics modeling was carried out in COMSOL software package, version 5.3. a three-dimensional model of the TEG was developed first. A parametric approach was considered for defining the connections between different geometric features of the model. In this way, it would be simpler to alter and investigate the effect of various geometries only by applying

the change in the desired features. Figure 3.7 shows the arrangments of the printed thermoelectric traces on the flexible substrate. T_l, L, and W are the thermoelectric legs thickness, length, and width, respectively. The rest of the geometric features and material properties are indicated in Table 3.1. Conducting polymer (PEDOT: Tos + TDAE) was chosen as the p-type thermoelectric material, and its thermoelectric properties were applied during the multiphysics modeling. For the n-type printed traces, an imaginary material with the same thermoelectric functions as PEDOT: Tos was considered for the modeling.
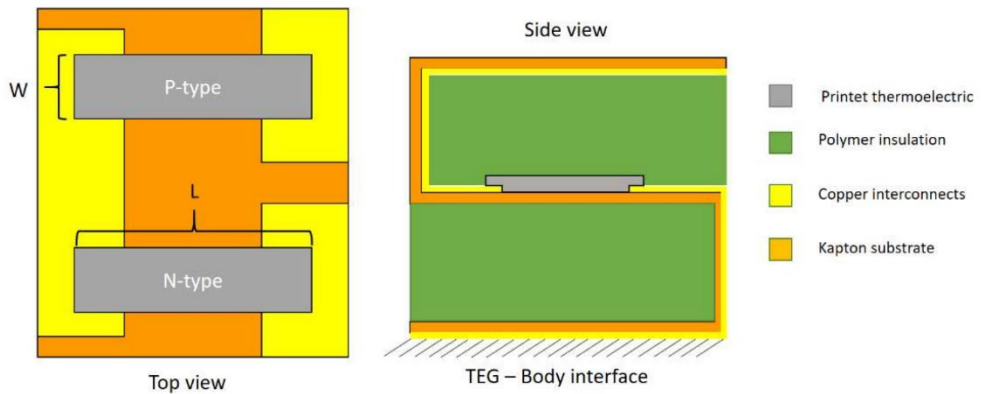

Fig. 3.7: Schematic of the proposed printed structure [22].

Table. 3.1: Schematic of a flexible thermoelectric generator [22].

Parameter	Symbol	Value
Seebeck coefficient (p/n-type)	$S_{p/n}$	± 215 μV/K
Electrical conductivity (p/n-type)	$\sigma_{p/n}$	70 S/cm
Thermal conductivity (p/n-type)	$k_{p/n}$	0.37 W/m-K
Hot side temperature	T_H	304.65 K
Ambient temperature	T_A	293.15 K
Natural heat transfer coefficient	h_A	5.46 W/m²-K
TE Leg length	L	12 mm
TE leg width	W	2 mm
TE leg thickness	T_l	150 μm
Copper interconnects thickness	t_1	100 μm
Thickness of Kapton substrate (polyimide)	T_k	25 μm
Thermal conductivity of interconnecters (copper)	K_{cu}	400 W/m-K
Thermal conductivity of Kapton (polyimide)	K_s	0.12 W/m-K
Electrical conductivity of interconnects	σ_{cu}	5.998×10^7 S/m

The 3D model is numerically solved in the next step by using COMSOL 5.3 default thermoelectric modeling module [22]. The finite element method is carried out to compute the value of the temperatures and electric potentials. The thermoelectric module design features are listed in the table, which contains the geometric parts, material specification, and boundary conditions. This simulation was considered for placing the thermoelectric generator on human skin. The heat transfer value from the cold side part is determined from the ANSI/ASHRAE Standard 55. In this case, it is equal to 5.46 W/m^2.K and happens due to the natural convection from the device's cold side without using a bulky heat sink. Figure 3.8 indicated the temperature distribution across the whole device after applying the mentioned boundary conditions.

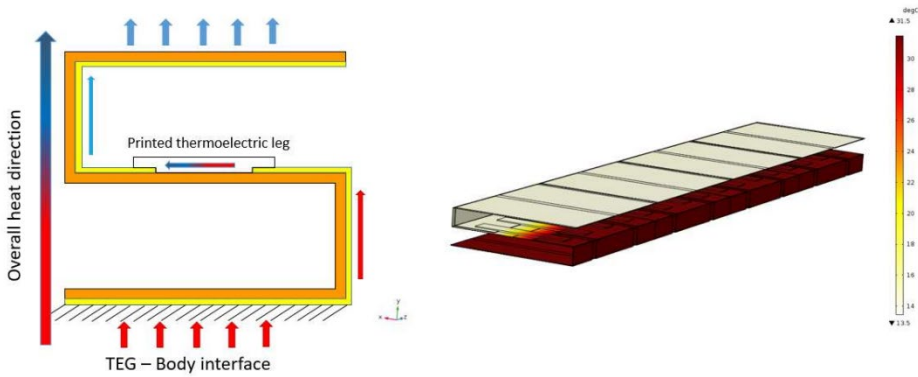Fig. 3.8: Heat distribution profile for folded printed TEG [22].

Figure 3.9 illustrates the TEG circuit. In this figure, V_D shows the amount of generated electrical potential, which leads to an electrical current of I_D inside the circuit. $R_{external}$ is the external resistance, R_{teg} is the thermoelectric generator's internal electrical resistance, and V_O presents the open-circuit voltage.
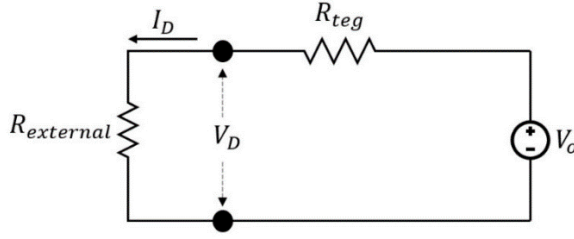
Fig. 3.9: Equivalent circuit for a typical TEG [22].

The value of the generated power can be calculated as follows [22]:

$$P_D = V_D \, I_D = \frac{V_D{}^2}{R_{external}} = \frac{\left[\dfrac{V_O \, R_{external}}{R_{external} + R_{teg}} \right]^2}{R_{external}} \qquad (3-1)$$

The maximum amount of power occurs when the external load's value is equal to the device's internal resistance. The amount of maximum power can be determined as follows [22]:

$$P_{max} = \frac{(V_o)^2}{4R_{teg}} = \frac{[n(s_p + s_n)\,\Delta T]^2}{4n\,(r_p \frac{L}{A} + r_n \frac{L}{A})} \qquad (3-2)$$

In the equation (3-2), r_n and r_p are the n- and p-type elements' electrical resistivities, A is the cross-sectional area, and L is the legs' length, respectively. These equations show the dependency of the TEGs output power to the geometric features such as the thermoelectric leg's length, width, and thickness. Based on this fact, it is possible to optimize the TEG overall performance by altering the mentioned geometrics features in the COMSOL 3D model and investigating their effects on the output power and voltage. In this direction, four values 75, 150, 300, and 450 µm were considered for the thermoelectric leg thickness, and a comparison was made between them in Figure 3.10 (a). The same approach was repeated for different thermoelectric legs length 9, 12, 15, and 18 mm, and the amount of their corresponding output power and voltage are shown in Figure 3.10 (b). Based on these simulations, the TEGs output power was increased by adding the thermoelectric legs' thickness and decreased by increasing the thermoelectric legs' length. This is due to reducing the TEGs internal resistance in the first case and rising the TEGs internal resistance in the second case, which is also predictable based on the Equation (3-2). In the second scenario, the effect of the changing of the legs width was examined by considering two conditions.

First, assuming that the number of the thermoelectric legs is fixed and in the second case, the number of the thermoelectric legs increased by decreasing the width. In the first case, Figure 3.11 (a), the amount of output power was increased by adding the legs' width due to the legs larger cross-section area and less electrical resistance. In the second case, Figure 3.11 (b) adding the number of legs by decreasing their widths resulted in higher open-circuit voltage. Still, at the same time, less output power was achieved because of the larger TEGs internal resistance.

By utilizing the COMSOL Multiphysics modeling and altering various design features, the printed flexible TEGs can be further optimized for different application scenarios in the future.
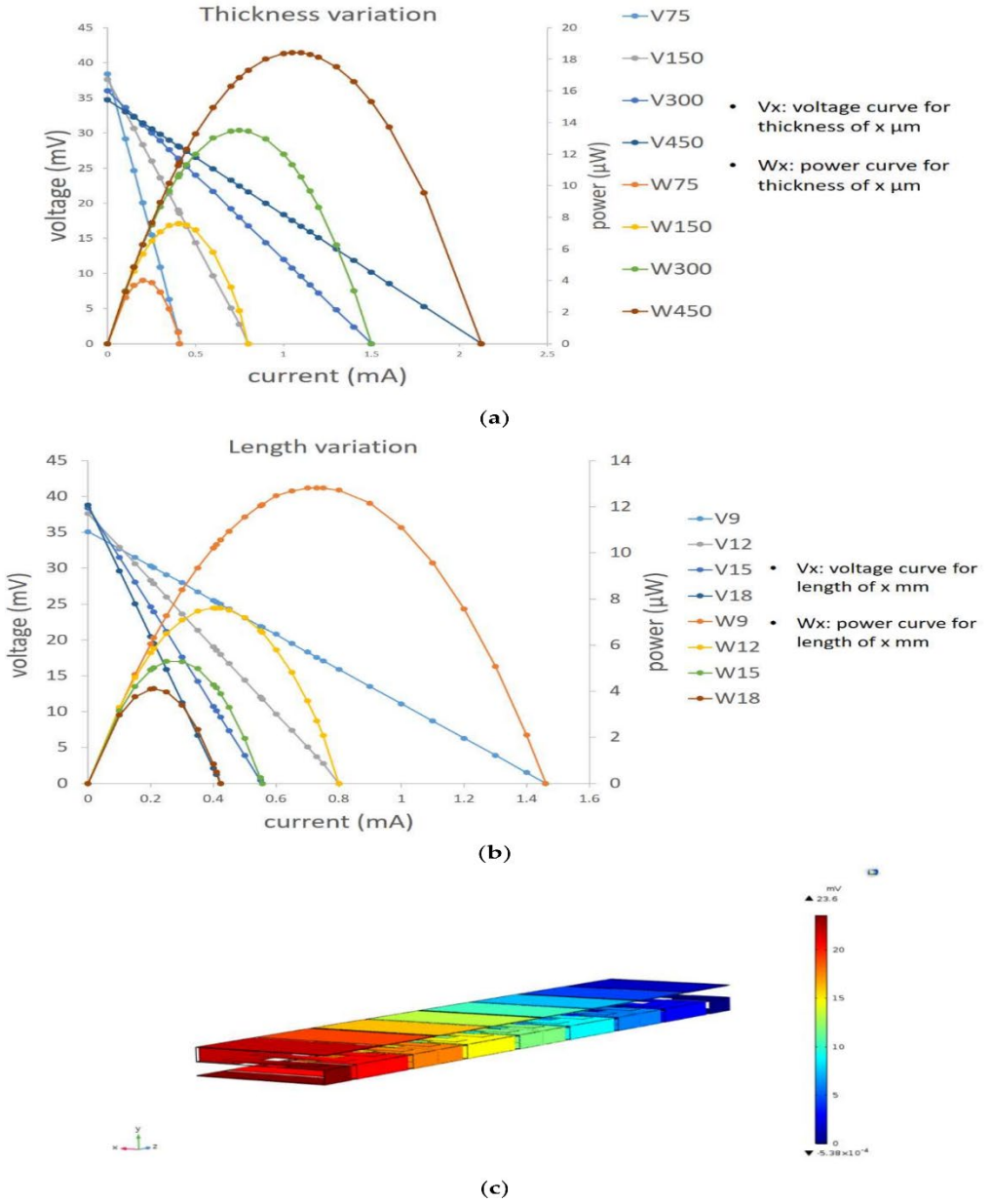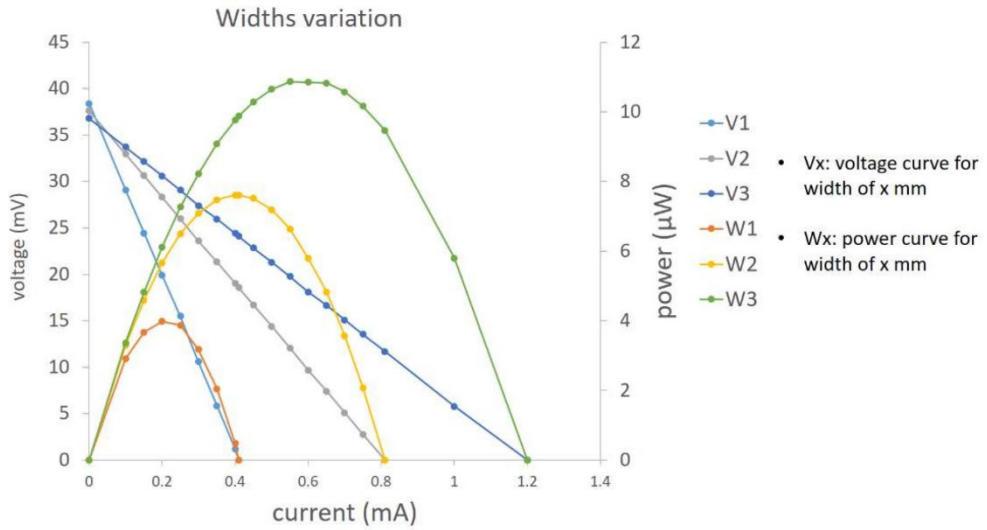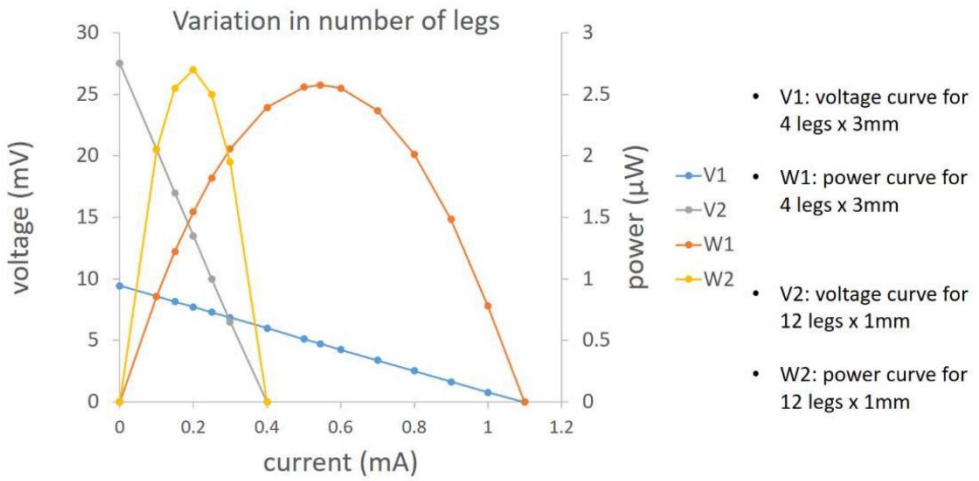
Fig. 3.10: (a) Effect of different leg thickness, (b) changing the length of the legs, (c) output voltage profile [22].

(**a**)

(**b**)

Fig. 3.11: (a) Effect of different leg's width, (b) changing the number of the legs [22].

CHAPTER 4. FLEXIBLE ZINC ANTIMONIDE THIN-FILM THERMOELECTRIC GENERATORS

Today Bismuth Telluride is the main thermoelectric material that is vastly used in commercial thermoelectric modules. But the high cost, existing in the list of the rare earth elements, and toxicity of this material are considered significant thermoelectric implementation challenges. As a result, there have been many attempts in the thermoelectric research community to find efficient alternative materials to tackle these barriers. In this direction, binary zinc-antimony materials (ZnSb and β-Zn4Sb3) have been attracted much attention as a cost-effective and relatively nontoxic p-type thermoelectric material for the medium temperature range (up to 350 °C) applications. It is also possible to further decrease the zinc-antimony based modules' cost by using the thermoelectric materials in the form of thin-films. But proper strategy should be taken into account to design and fabricate thermoelectric modules using thin-films for real-world applications. This chapter begins with zinc antimony thin-films fabrication through magnetron co-sputtering. Then two methods are introduced to fabricate flexible thin-film devices.

4.1 MAGNETRON CO-SPUTTERING OF ZINC ANTIMONIDE THERMOELECTRIC THIN-FILMS

As mentioned in chapter two, the functional materials typically can be deposited by two different sputtering techniques, direct-current (DC) sputtering and radio-frequency (RF) sputtering. They are using the same type of features inside the vacuum chamber, but the power sources are various. The ability of deposition on an insulating target substrate is also applicable only through RF sputtering. In magnetron co-sputtering, a magnetic field is imposed to enhance the deposition rate and increase the deposited layer's quality. Different parts of a magnetron co-sputtering are illustrated in Figure 4.1. a permanent magnet is placed behind the target to generate a parallel leakage field exiting the substrate surface. This

magnetic field causes an efficient ionization effect even at a lower gas pressure range, which provides a higher deposition rate. It has also been claimed that by combining Ar gas with H_2, deposited thermoelectric film obtains better thermoelectric functionality [73]. This enhancement is due to the raising of the number of charge carriers and the film's electrical conductivity.
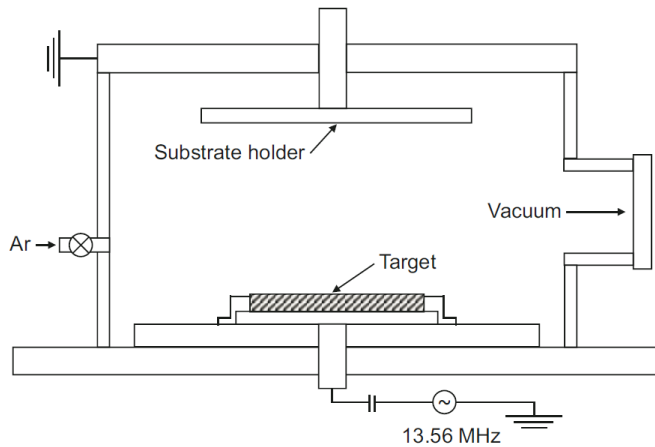
Fig. 4.1: Typical magnetron co-sputtering [53].

In this work to fabricate a flexible thin-film based thermoelectric generators, thin-films of ZnSb were prepared by magnetron co-sputtering deposition. The silica wafers were utilized as the substrate material with a thickness of 350 μm. In order to achieve high-quality crystallization, the substrate was kept at 215 °C at the time of the sputtering process. Inside the chamber, Argon with a purity of 99.9996% applied. The deposition was done in 60 min. Two target materials were used, Zn_4Sb_3 set at 12W and Zn set at 4 W. the pressure inside the chamber had an estimated value of 3×10^{-5} Pa. the samples then heated up to 300 °C with a heating rate of 100 °C h^{-1} within 2 hours in the air. Powder X-ray diffraction (PXRD) was used to validate the phase transitions in the films. The films' characterization was carried out by EM with EDX, PXRD was collected on a Rigaku Smartlab 9 kW rotating anode Cu-K$_\alpha$ source, parallel beam optics in θ–2θ geometry. The SEM image was used to determine the 600 nm thickness of the film. The atomic ratio of the Zn:Sb is shown in Table 4.1. indicates the PXRD pattern and theoretical data set from LeBail fitting.

Table. 4.1: Atomic ratio in the deposited film [26].

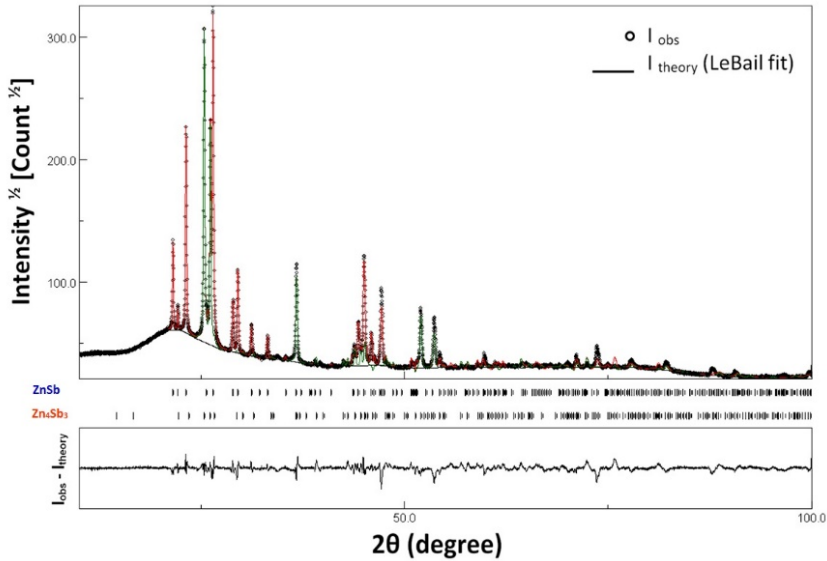| % (Zn)	% σ (standard deviation of Zn)	% (Sb)	% σ (standard deviation of Sb)
57.6	1.8	42.4	1.3

Fig. 4.2: PXRD pattern of the deposited film [74].

4.2 FABRICATION OF FLEXIBLE THERMOELECTRIC GENERATOR WITH THIN-FILMS OF ZINC ANITIMONIDE

Here, zinc antimonide thin-films are integrated into the two different flexible device design concepts. Four p-type ZnSb thin-film pieces and four straps of constantan were used to form the final module architecture. Constantan was selected due to the lack of comparable n-type material to the zinc antimonide film. They are also flexible and have a small thermal conductivity, which is beneficial in a flexible thermoelectric generator. In both cases, nanosilver paste was chosen to join different specimens and attach thin-films at a flexible substrate. The reason for selecting this bonding technique over soldering is that nanosilver bonding can tolerate a higher temperature range. This is crucial for ZnSb thermoelectric generators, which have operational temperature ranges beyond the soldering materials' melting point.

The first flexible thermoelectric generator (FTEG1) contains four thin-films and four constantan straps, directly joining without using any holding substrate. The edge of each constantan strap is bonded to the films through silver sintering (Figure 4.3 (c)). To avoid short circuits between the straps and adjacent films, they were covered by a layer of Kapton from one side. This configuration can only handle a small degree of bending and mechanical force. In the second flexible thermoelectric generator (FTEG2) concept, a flexible carrier substrate was implemented to enhance the module's flexibility and mechanical stability. First, the nano-silver bonding material was deposited on the Kapton carrier substrate employing a desktop PCB printer. Then the thin-films of ZnSb and constantan straps were placed at the dispensed bonding material for joining (Figure 4.4 (a)). This step can be replaced by an automatic pick and place in a large-scale manufacturing scenario. The bonding step was completed by heating up the joints to 200 °C for 30 min. P-types and constantan straps were connected by copper electrodes from the other side using nano-silver paste (Figure 4.4 (b)). They were cut and formed in a specific shape at the cold side of the FTEG2 in order to act as a small heat sink at the same time (Figure 4.4 (b)). Figure 4.4 (c,d). shows that the FTEG2 can easily be bent and withstand more mechanical forces than the FTEG1. This fabrication method can be scaled up for large volume production by utilizing printing methods for joining material deposition and automatic pick and placing.

a

b

c

d
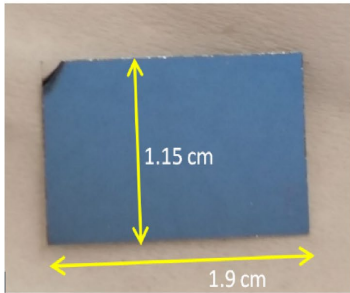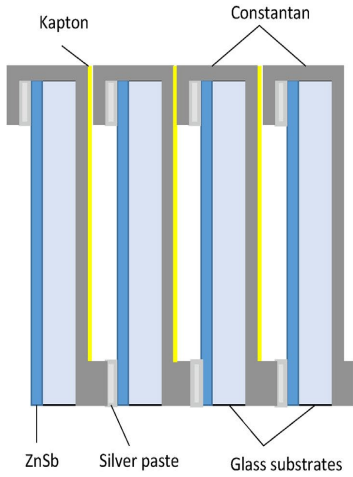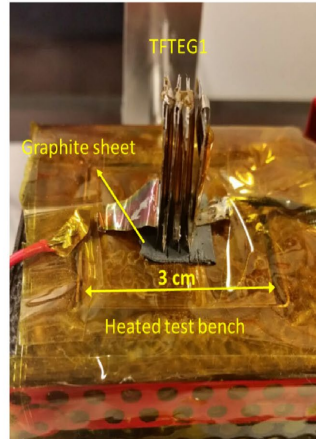
Fig. 4.3: FTEG1 fabrication: (a) ZnSb thin film, (b)device components, (c) bonding, (d) FTEG1 charactrization [74].
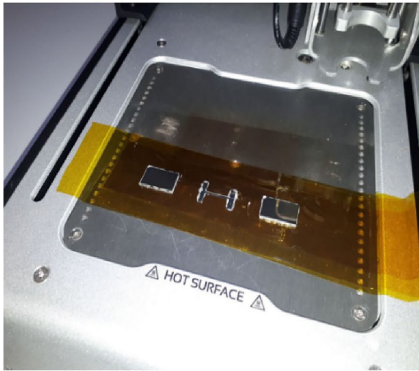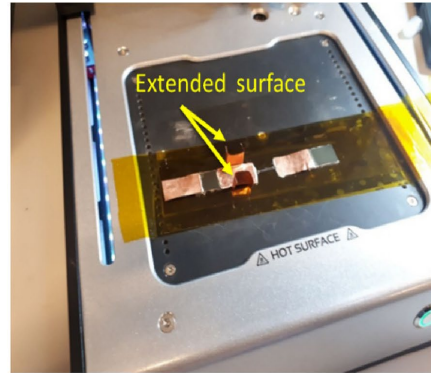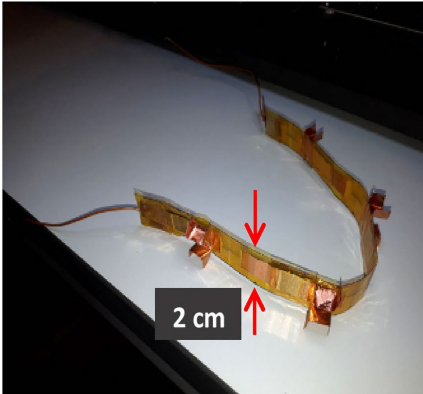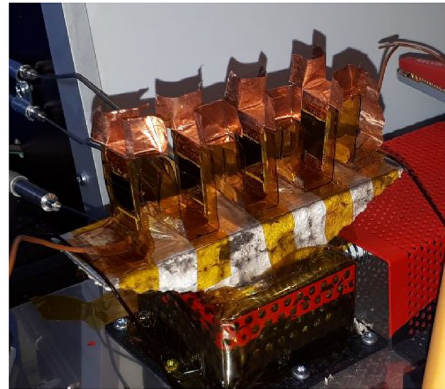
Fig. 4.4: FTEG2 concept: (a) ZnSb bonding to the flexible substrate, (b) attaching the copper electrodes and extended surfaces, (c) final assembles FTEG2, (d) FTEG2 installed in the characterization setup [74].

Both devices were characterized for examining their thermoelectric functionalities at various hot side temperatures. The FTEG1 first was fixed at the test bench hot plate (Figure 4.3 (d)) and heated up to different temperatures. External electrical resistance was imposed to achieve the power output curve. For any set hot side temperature, holding time was considered to obtain a thermally stable situation. Based on the achieved results, the maximum power for FTEG1 happened at the external load among $100 \, \Omega$ and $150 \, \Omega$. The maximum power of 13.5 μW occurred at 330 °C for the hot side of the FTEG1. The open-circuit voltage versus the

temperature of the hot side is shown in Figure 4.5 (b). according to the experiment results, the FTEG1 proved to be functional at temperatures up to 330 °C. The FTEG2 was also tested following a similar approach, and the obtained results are illustrated in Figure 4.5 (c,d). based on the results, it can be seen that the second design has less amount of generated power compared to the FTEG1. This is mainly related to the negative effect of the Kapton layer's thermal resistance from the hot side interface. In the second design, copper electrodes were added to complete the FTEG2, which can also increase the value of the electrical contact resistance decrease the overall performance. The FTEG2 managed to generate a pick power of 3.5 μW at 250 °C. The proposed modules' performance can be further optimized by a more detailed investigation of the bonding sections' contact resistance. For example, sintering parameters like bonding temperature and holding time affect the final joints' function. It should be mentioned that introducing new n-type material that could be utilized instead of constantan straps enhances the overall efficiency of the FTEGs.

(a)

(b)

(c)

(d)
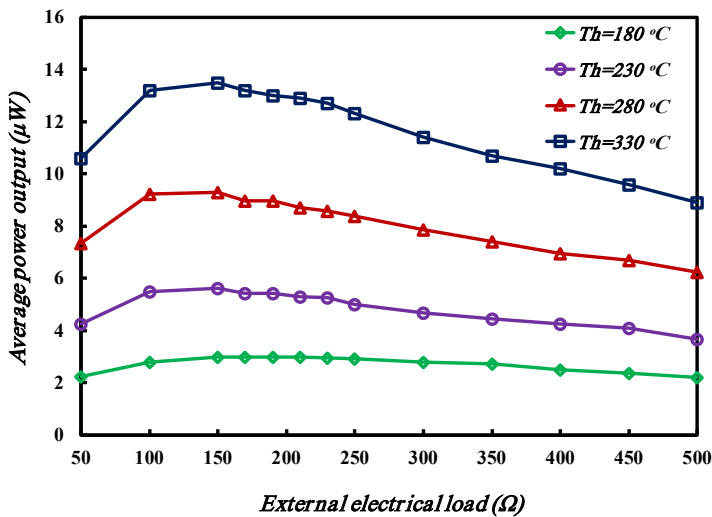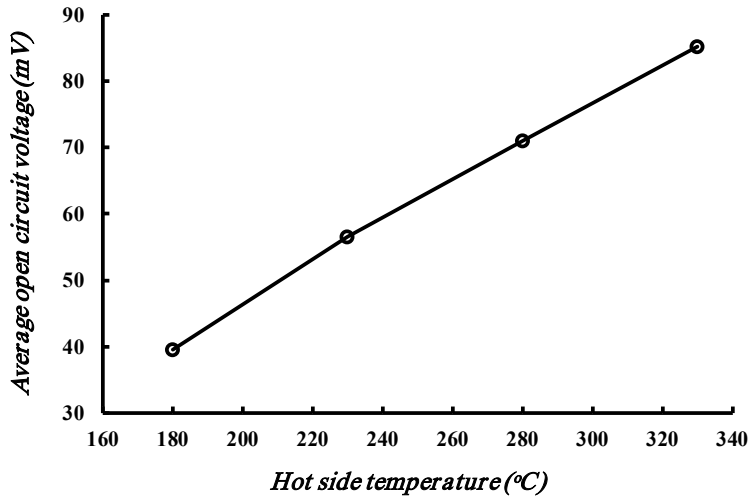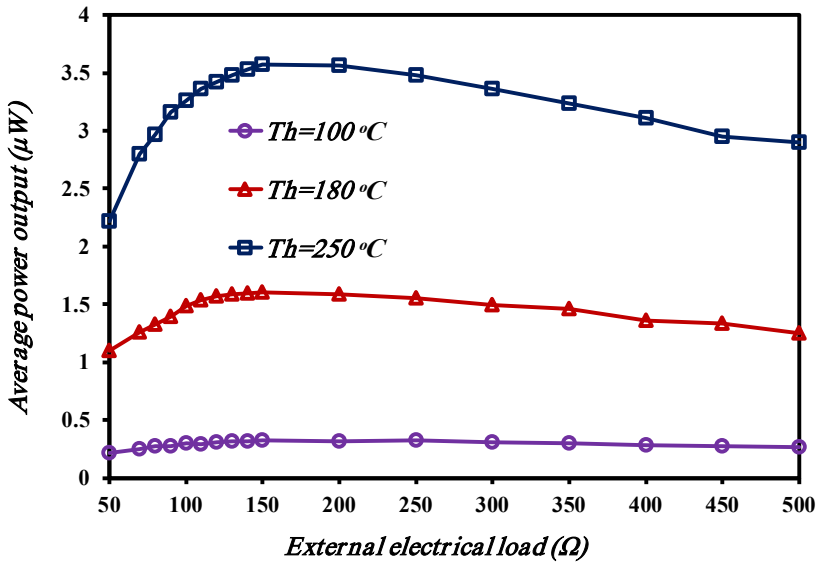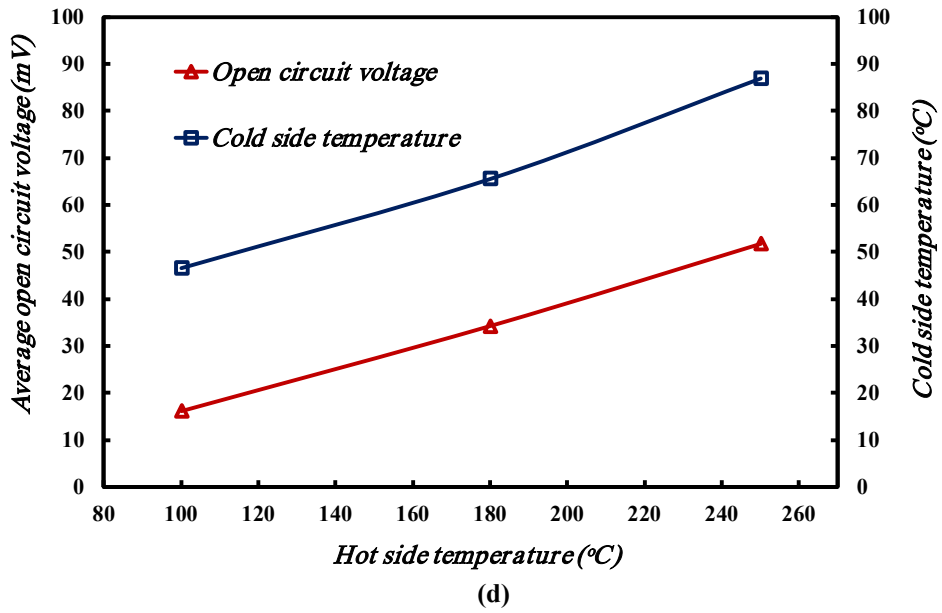
Fig. 4.5: a,c) Power, b,d) Voltage for FTEG1 and FTEG2 [74].

CHAPTER 5. FABRICATION OF FLEXIBLE THERMOELECTRIC GENERATORS USING BULK MATERIALS FOR LOW TO MEDIUM TEMPERATURE RANGES

Until now, bismuth telluride has been the main material in the manufacturing of commercial thermoelectric modules. It posses the highest thermoelectric conversion efficiency compared to other developed materials. Both organic and in-organic printable thermoelectric materials can not compete to BiTe in terms of efficiency and stable functionality. As a result, to achieve flexible thermoelectric generators that could be replaced with current commercial thermoelectric modules, one strategy could be trying to use the same bulk thermoelectric materials in a flexible supporting structure. In this chapter, a manufacturing concept is introduced for the high throughput production of flexible thermoelectric generators based on a method similar to the flexible hybrid electronics (FHE) concept. Nano-silver sintering was also applied for bonding, which enables the applicability of the flexible TEG at a higher range of temperatures.

5.1 HIGH THROUGHPUT MANUFACTURING OF FLEXIBLE THERMOELECTRIC GENERATORS WITH FLEXIBLE HYBRID ELECTRONICS

Many studies have focused on developing a flexible thermoelectric generator (FTEG) using bulk thermoelectric materials to have a comparable functionality with commercial TEGs. Yet, few of the proposed approaches have the capability of scaling up for large volume production. Here a manufacturing concept is proposed for high throughput manufacturing of FTEGs. This concept is based on additively adding the electrical interconnects on a flexible substrate to bond the pellets of thermoelectric materials. The idea is similar to flexible hybrid

electronics (FHE), which combines printed electronics and traditional silicon electronics. FHE provides bonding the rigid surface mount components like IC (integrated circuits) on flexible substrates, leading to both required flexibility and processing capability. Flexible printed circuit boards (FPCBs) have been the main technology in manufacturing flexible printed electronics. The main difference between FPCB and FHE is that in FPCB, flexible electrical conductors are not fabricated additively by printing conducting materials. They are normally made by etching a copper cladding flexible substrate, which is a subtractive approach for patterning the electrical interconnects. As a result, in FHE, the substrate's patterning can be performed with less material wastage due to the approach's additive nature. Besides, the additive method is more cost-effective in less dense circuits, as shown in Figure 5.1 For substrate with a smaller fill factor (ratio of the covered area by the electrical conductor material to the substrate's overall surface), FHE results in less material wastage and reduced total cost. Implementing high-speed deposition methods such as inkjet and aerosol printing in FHE can also significantly reduce the manufacturing time since there is no need for a mask for printing. Any changes in the flexible printed circuit design can be handled more agilely due to the interconnects' mask-less fabrication and digitally controlled material deposition. It is also possible to integrate the FHE into a high volume fabrication scenario, such as roll-to-roll printing, which can be happened with the FPCB method.

Figure 5.2 shows a one-stop-shop manufacturing concept based on FHE for the high throughput production of FTEGs. It starts with roll-to-roll patterning of flexible substrates with conductive printable materials. Then pellets of bulk materials are bonded to the printed interconnects through automatic high-speed pick&place step. A curing or sintering process should be considered afterward to complete the FTEGs fabrication based on the applied bonding method. In the final stage, proper reliability and functional tests should be designed and integrated into the manufacturing platform—these tests guaranty both thermoelectric functionality and mechanical flexibility of the FTEGs.
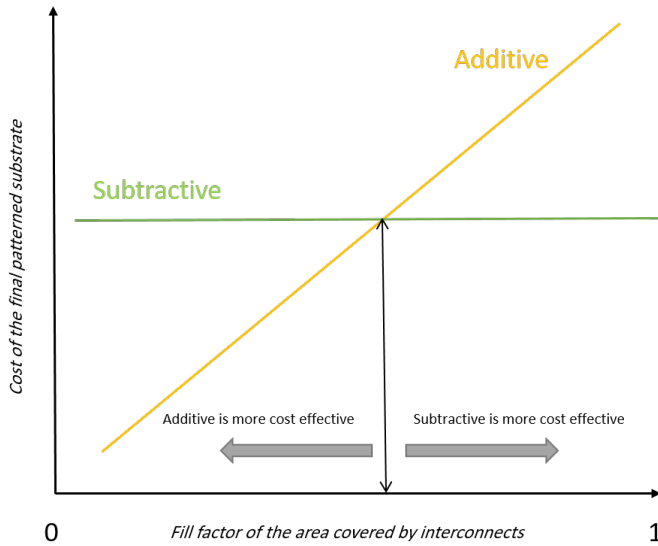
Fig. 5.1: Comparing of additive and subtractive approach for patterning the flexible substrate [75].
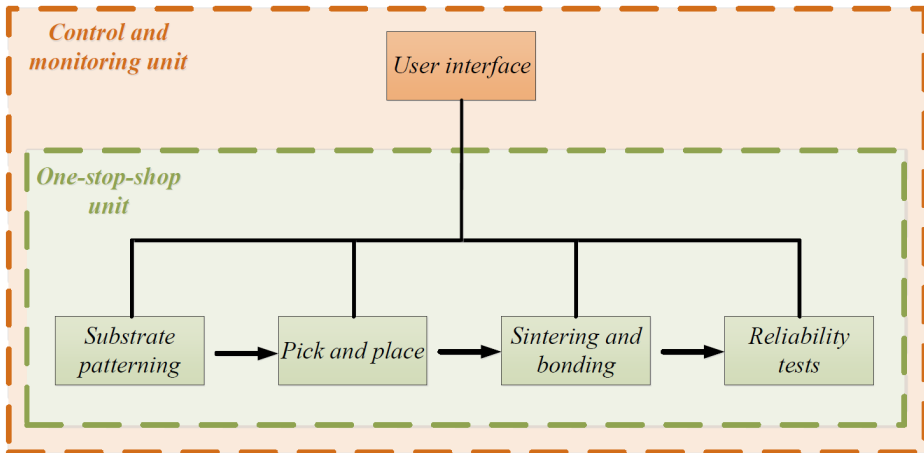
Fig. 5.2: One-stop shop manufacturing concept based on the FHE [75].

It is also worth mentioning that, by introducing novel printable thermoelectric material that could compete with bulk thermoelectric materials in thermoelectric functionality, the whole proposed method can be done additively. It means that the pick&place step would be replaced by a printing step, such as the direct writing of the thermoelectric materials (Figure 5.2). It could be accomplished through a high-speed dispensing technique like an electrohydrodynamic dispensing (EHD) valve, reducing the overall fabrication time and cost. This also brings a higher level of flexibility and agility for the manufacturing platform since the deposition process can be controlled digitally and on-demand, simplifying the adoption of any design and fabrication changes. However, to realize the high-speed deposition of printable thermoelectric materials, other parameters such as fine-tuning the material's rheology should be considered. Another advantage of printing is that the bonding material is not required since the thermoelectric materials are deposited directly on the electrical interconnects, decreasing manufacturing time, cost, and complexity. However, the interface between printed materials and electrical conductors should be carefully examined to have minimum electrical contact resistance and maximum mechanical bonding strengths.
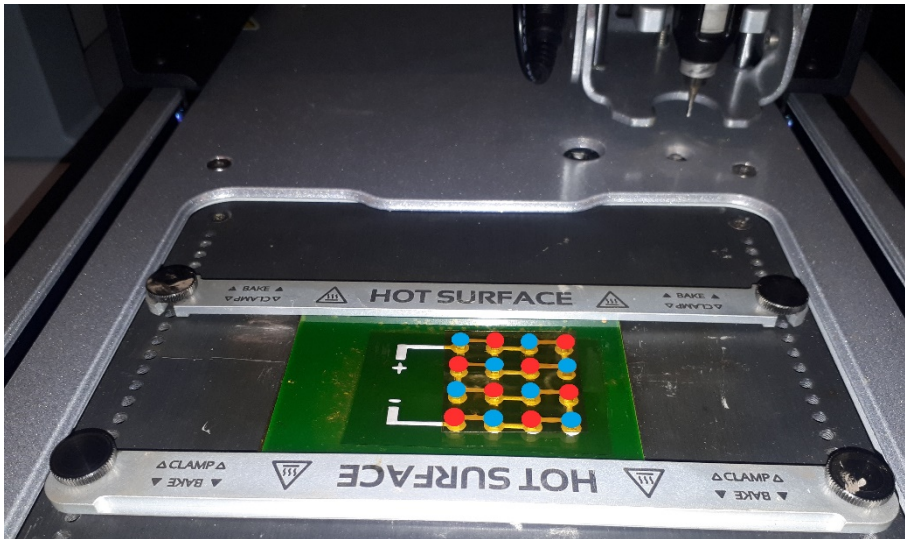
Fig. 5.3: Dispensing of printable thermoelectric materials, the blue circles represent the p-type, and the red circle represents the n-type [75].

5.2 FABRICATION OF FLEXIBLE THERMOELECTRIC GENERATORS USING NANO-SILVER BONDING

Here, the fabrication of a prototype is explained based on the last section's proposed manufacturing concept and nano-silver bonding. Figure 5.4 demonstrates the various prototyping steps. Thermoelectric materials were prepared in the form of cubic pellets (2mm × 2mm × 2mm). They were cut from a 2 mm thick bismuth telluride wafer (p- and n-type) and then diced through a wire cutting machine (Figure 5.4.(a).). The wafer was coated by a sputtered Nickel layer, which acted as a protective surface to avoid the bonding material's penetration into the thermoelectric pellets. As shown in Figure 5.4., the top and bottom electrodes were printed on a Kapton flexible substrate by a digitally controlled dispenser. As mentioned in the previous section, fabricating the electrodes additively can reduce the amount of material consumption, increase the fabrication agility, and decrease the total fabrication time and cost.
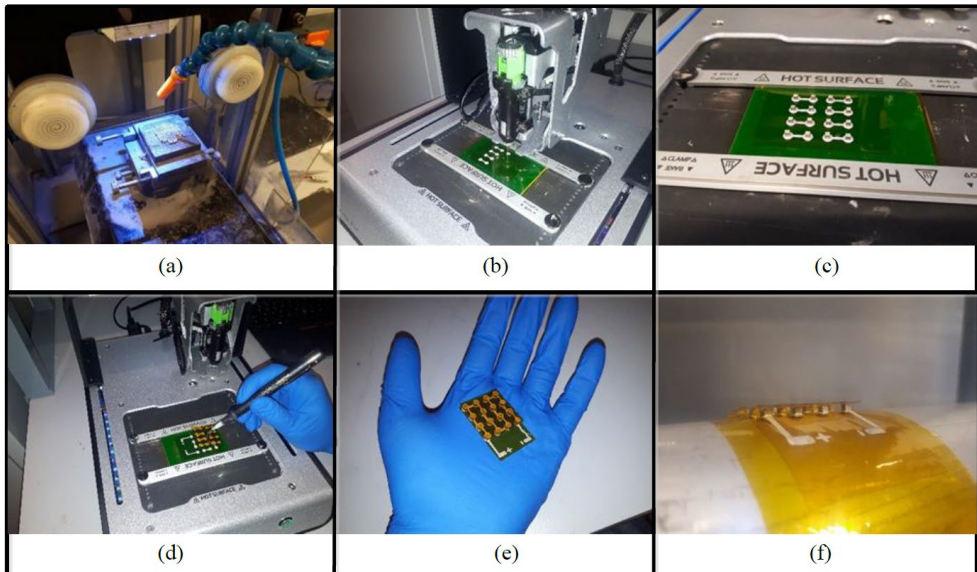
Fig. 5.4: Flexible TEG fabrication steps. (a) dicing the bismuth telluride wafer, (b) dispensing the electrode materials, (c) pick&place and bonding, (d) final assembly – top and bottom layer, (f) flexible TEG placed on a curved surface [75].

The pellets were picked and placed on top of the printed electrodes and joined to the flexible substrate by nano-Ag (silver) bonding. Nano-Ag bonding containing silver nanoparticles with a melting point of 926°C for silver can tolerate higher temperatures than the solder bonding, such as SnCu (227°C) or SnSb (232°C). Unlike the solder reflowing, no liquid phase is made during the sintering process in the nano-Ag bonding [76]. As a result, the bismuth telluride pellets can be fixed more convenient with less slipping during the bonding step. The printed electrodes and pellets on top of them were then heated to 210 °C for 30 minutes to complete the bonding. In this way, there is no need for additional bonding material since the printed electrodes act as the bonding material as well. It is also possible to alter the bonding sections' characteristics by adjusting the sintering time and temperature [77]–[80], which is not part of the current study. It is also worth mentioning that the silver sintering results in bonding parts with much higher thermal conductivity (200 to 300 W/mK) and less electrical resistivity (2.5 and 10 μΩ.cm) compared to the solder joints. As a result, the TEGs can provide greater thermoelectric functionality at higher operational temperature ranges.

5.3 EXPERIMENTAL RESULTS AND DISCUSSION

In order to examine the prototype performance at various temperatures and under the bending conditions, two sets of tests were considered. These tests were started by monitoring the generated voltage and power at different hot side temperatures and recording the device's internal resistance changes due to cyclic bending conditions.

5.3.1 OUTPUT POWER AND VOLTAGE

Figure 5.5 shows the characterization setup of TEGs used in this study. The setup can impose various temperature differences to TEGs through an electrical heater at the hot side and a liquid cooling system from the cold side of TEGs. TEGs are placed between the two stainless steel cubic blocks. Each block has four spots for inserting N-type thermocouples to capture the temperatures (Figure 5.5. (b)). For each temperature difference, various external electrical loads can be set in order to extract the corresponding voltage-current (V-I) and power-current (P-I) curves. The setup also provides a vacuum casing that can decrease thermal parasitics and enhance the test's accuracy. The flexible TEG was clamped into the setup and tested for different hot side temperatures.
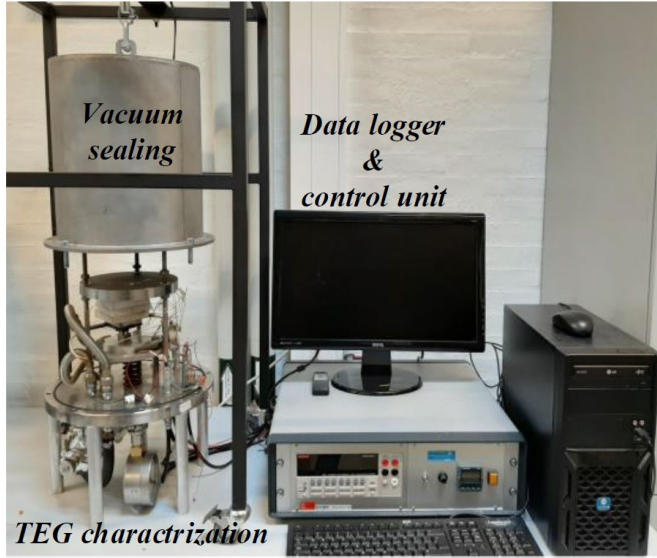
(a)
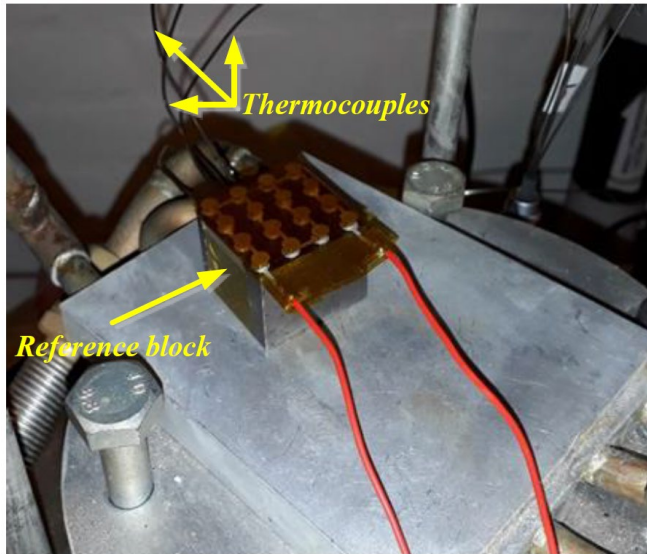
(b)

Fig. 5.5: (a) TEG characterization setup, (b) FTEG attached to the reference blocks, and thermocouples [75].

The results are elaborated in Figure 5.6 and showed that the nano-Ag bonding could withstand temperatures as high as 278 °C. Surprisingly, the power output of the FTEG was doubled from 45 mW to 88 mW when the hot side temperatures increased from 187 °C to 278 °C. This enhancement in power output happened even though the Seebeck coefficient of bismuth telluride has a fast reducing behavior for the temperature ranges over 200 °C [81]. This enhancement is due to the increasing of the heat flux across the device at higher temperatures, which justifies utilizing efficient bonding techniques such as silver sintering.

(a)

(b)
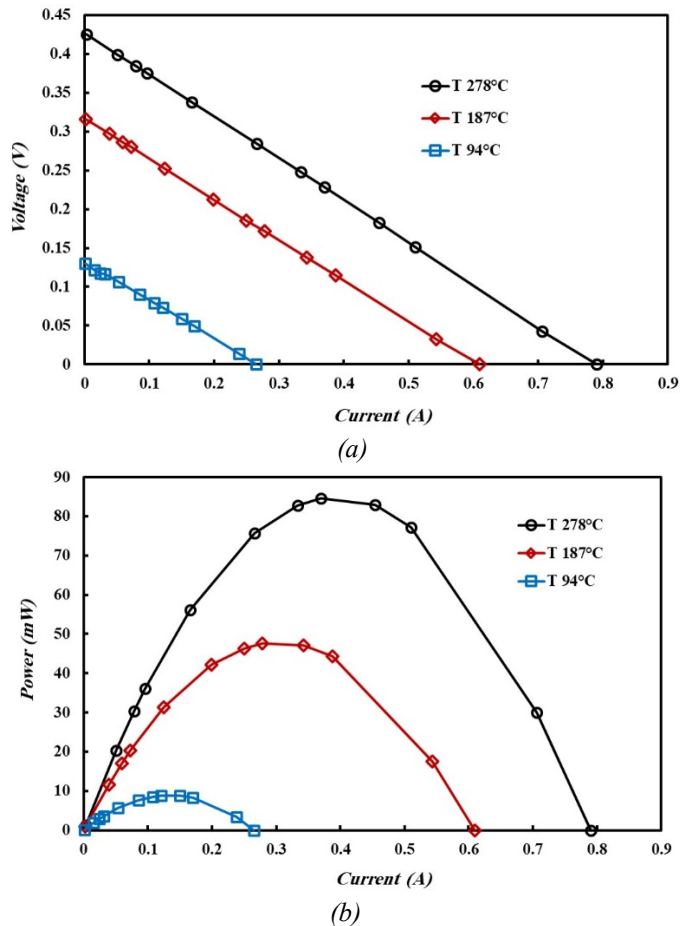
Fig. 5.6: (a) Voltage versus current, (b) Output power versus current [75].

Figure 5.7 shows the equivalent circuit of a TEG where V_{TEG} is the device potential, I_D is the electrical current flow, R_{TEG} is the device internal resistance, and R_{EXT} is the electrical load applied by the characterization setup. The open-circuit voltage is achieved as follows [75]:

$$V_{OC} = \alpha \times \Delta T \qquad (5-1)$$

Where α equals the device Seebeck coefficient. The internal resistance of the TEG can be calculated as follows [75]:

$$R_{TEG} = \frac{R_{EXT} \times (V_{OC} - V_{TEG})}{V_{TEG}} \qquad (5-2)$$

When the amount of the external applied load (R_{EXT}) becomes equal to the amount of the device internal resistance (R_{TEG}), the maximum power of the TEG is obtained, which can be formulated as follows [75]:

$$Pmax = \frac{V_{OC}^2}{4R_{TEG}} \qquad (5-3)$$

The FTEG had a resistance ranged between 0.45 to 0.55 ohm considering the results obtained from the tests. Figure 5.8 shows the maximum output power and open circuit voltages versus temperature differences across the device. It can be concluded that the amount of temperature differences has determined the FTEG´s performance as the main factor. The same is valid for temperatures higher than 200 °C despite reducing the bismuth telluride thermoelectric properties.
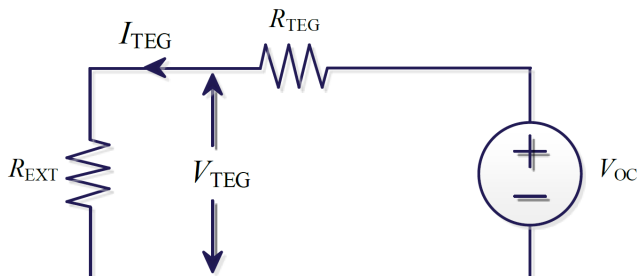
Fig. 5.7: TEG electrical circuit [75].
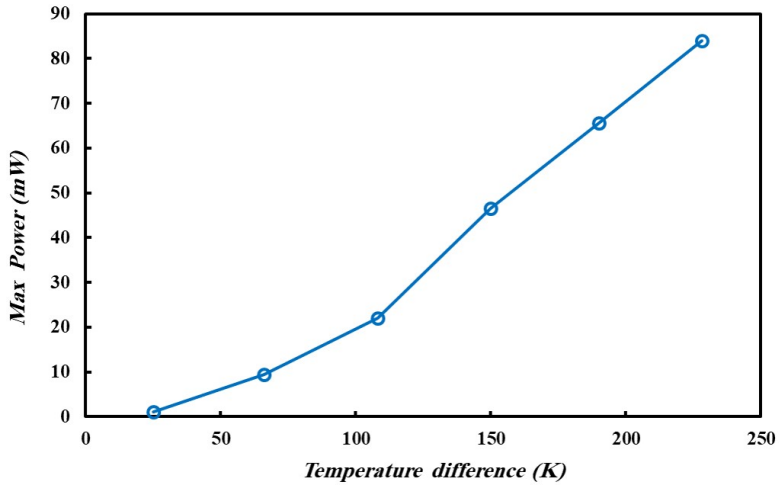
(a)
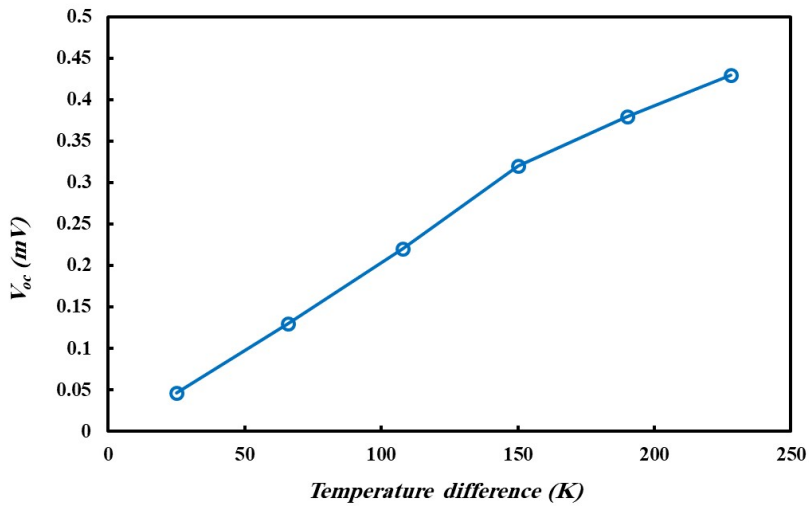
(b)

Fig. 5.8: (a) Maximum output power versus temperature differences across the FTEG, (b) open-circuit voltage for various temperature differences [75].

5.3.2 BENDING TESTS

In order to examine the performance of the FTEG under the bending conditions, a cyclic bending test was carried out. The device was then mounted on a curved surface and heated by a flexible heater to monitor the amount of open-circuit voltage.

The cyclic bending test is normally conducted to prove the flexible printed electronic devices' reliability by imposing a cyclic mechanical load at various bending curvatures. The device is bent for a specific number of bending cycles, and the performance change is monitored. In the case of FTEGs, the same method can be applied to investigate the bending reliability. Here the FTEG was bent for100th, 200th, 500th, and 1000th bending cycles, and the change in the device internal resistance was captured. For applying the cyclic bending loads, the FTEG was fixed into a clamp to be bent with different bending diameters, 30, 40, and 60 mm (Figure 5.8.). The device resistance change can happen due to the printed electrodes' delamination and the bonding sections' failure. The Z-meter (DX4095 Peltier Z-Meter, TEC Microsystems GmbH) was used to measure the FTEG internal resistance. Figure 5.9. indicates the cyclic bending test results, which shows a small variation in the FTEGs internal resistance.
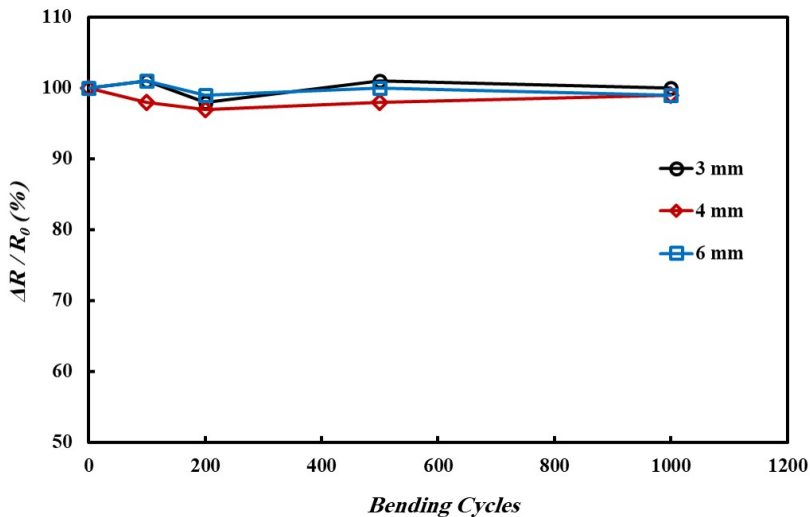
Fig. 5.9: Cyclic bending test [75].

The FTEG was also attached to the outer surface of a pipe and heated, employing a flexible heater for demonstration (Figure 5.10). Simultaneously, the open-circuit voltage was recorded to show the functionality of the FETG, and the results are shown in Figure 5.11.

The FTEGs managed to show functionality on the curved surface, and the amount of open-circuit voltage was increased by raising the hot side temperatures.
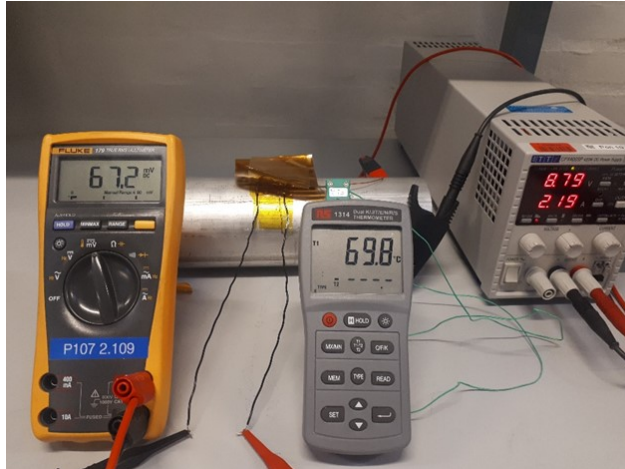
Fig. 5.10: FTEG attached at the curved surface [75].
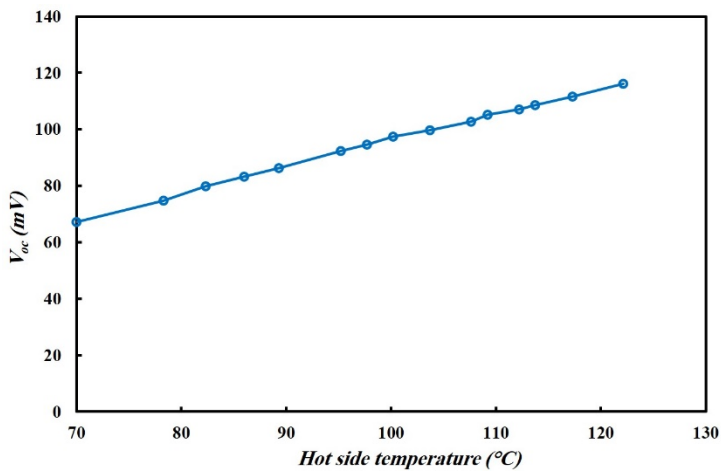
Fig. 5.11: changing the open-circuit voltage versus hot side temperatures [75].

CHAPTER 6. CLOSURE

This chapter presents a summary of the study conducted in the form of the Ph.D. thesis. It draws a roadmap for the future development of manufacturing methods to mass production of flexible thermoelectric generators.

6.1 CONCLUSIONS

A review of the current manufacturing technologies for the fabrication of thermoelectric generators and developing a concept for mass production of these modules are presented and studied in this dissertation:

For printed thermoelectric generators:

There are many printing methods for the fabrication of thermoelectric generators. These techniques can be categorized based on their approach for deposition of thermoelectric material, accuracy, applicability for high throughput fabrication, and manufacturing speed. These techniques provide an additive platform for the fabrication of thermoelectric generators; however, specific printable thermoelectric material should be designed for each approach due to the various deposition mechanisms. Among the printing techniques, screen printing shows the most promising potential for large volume fabrication. The technique has already matured for other printed electronics products because of the system's simplicity and great fabrication rate. Dispenser printing is also another promising method for the deposition of functional materials, but the main drawback is the low deposition speed. It is also possible to make a 3D stack of functional materials with dispenser printing, which enables to print of the vertical configuration thermoelectric generators. Printable thermoelectric materials have less thermoelectric functionality than their commercial inorganic counterparts since most of them are based on organic thermoelectric materials with poor thermoelectric specifications. However, the printable materials contain inherently less expensive and earth-abundant elements, providing a much higher mechanical flexibility and solution processability level. A multiphysics modeling for planar printed flexible TEGs was applied for design optimization. The proposed design for the planar TEGs included a heat-conducting path made by folding the flexible substrate in desired spots. The concept of printing and folding can be utilized for large volume products such as roll-to-roll.

For flexible thin-film thermoelectric generators:

Due to the significantly less amount of material consumption in thin-film-based devices, the overall consumed thermoelectric material's cost reduces dramatically. Besides, they pose higher power per unit area compared to the bulk material. They also ideal for miniaturization, which is an important factor for powering remote sensors and IoT (internet of things) applications. Most of the works in this area have been focused on developing thin-films of bismuth telluride by various deposition methods. Alternatively, zinc antimonide shows promising performance as a p-type thermoelectric material, specifically for the medium-range waste heat recovery applications. Thin-film of zinc antimonide can be fabricated by sputtering techniques on the different carrier substrates. However, lacking an equivalent n-type for zinc antimonide makes it difficult to unlock this promising material's potential in the form of a complete device. At the device level, there should be a consideration for the design and fabrication of thin-film-based TEGs because the thickness of the functional thermoelectric layer is minimal, and maintaining the temperature difference across the whole device is challenging. Two concepts were proposed to fabricate flexible TEG by using zinc antimonide thin-films as the p-type and straps of constantan as the n-type material. Silver sintering was used for bonding to tolerate the higher temperature ranges. In the second proposed fabrication, a flexible carrier substrate was used to provide more mechanical flexibility and scalability for large volume production. Thin-film TEGs could be scaled up for large volume production by utilizing the high throughput sputtering methods.

For flexible bulk thermoelectric generators:

Although printed TEGs are promising for large volume production, yet they suffer from low conversion efficiency compared to conventional bulk thermoelectric materials. As a result, one strategy could be fabricating flexible TEGs using the same bulk material as the commercial TEGs. In this direction, a manufacturing platform was proposed for the high throughput fabrication of flexible TEGs based on the concept of flexible hybrid electronics. It offered a combination of automated pick&placing and additive printing of electrical electrodes. All the fabrication steps can be accomplished on a one-stop-shop concept, which brings flexibility and agility to the whole process. In the next step, prototypes were fabricated based on the proposed manufacturing concept. Nano-silver sintering was used to bond between the pellets of bismuth telluride and flexible substrate, which could tolerate higher temperatures than the soldering. In this way, a higher amount of power can be achieved due to the availability of the higher temperature differences at hot side temperatures above 200 °C. A cyclic bending test was carried out, which proved the prototypes' reliability under the bending condition.

6.2 OUTLOOK

The following suggestions can be applied for further investigation and development of new manufacturing methods based on the study carried out in this study:

Regarding printed flexible TEGs:

- New printable materials should be developed, which could compete with conventional bulk thermoelectric materials. These materials may be polymer-based, inorganic, or hybrid (a combination of organic and inorganic).
- In addition to thermoelectric functionality, any new printable materials should comply with high rate deposition and printing situation. This requires investigating the printability of these material parallel to their conversion efficiency and concerning different printing techniques.
- In the design part, there are great possibilities for introducing novel concepts for printed TEGs. This could result in decreasing the gap between the power output of bulk inorganic TEGs and printed TEGs.
- Most of the attempts have been focused on planar printing devices, while vertical printed TEGs can be utilized conveniently at system-level installation. As a result, customizing printing methods that could build vertical structures seems necessary.
- New printing methods such as high speed dispensing can be further explored since they offer high-speed deposition of the functional materials that can be controlled digitally. Hence, the agility of manufacturing will increase, and the material wastage would be minimal.

Regarding thin-film flexible TEGs:

- The deposition methods should be more studied to be customized for large volume deposition scenarios.
- More research should be performed in the development of thin-films with novel materials in addition to the bismuth telluride. For example, the focus could be on cheaper and air abundant materials.
- For medium temperature applications, zinc antimonide has promising performance, but developing proper n-type material with the same degree of efficiency is necessary.
- The effect of various carrier substrate should be further investigated, with the final aim of fabricating thin-films directly on a flexible substrate.

Regarding bulk flexible TEGs:

- The electrodes were additively added to on flexible substrate instead of subtractive approaches like etching in flexible printed circuit boards (FPCB). This can lead to a significant reduction in the cost and time of manufacturing. Besides, each change in the electrodes' pattern can be simply handled by changing the printing pattern digitally. Yet the printed electrodes can not compete with the etched copper electrodes in FPCB in terms of electrical conductivity. As a result, any development in the area of conductive ink can result in increasing the FTEGs efficiency with printed electrodes.

- Silver sintering requires a more detailed study for broader utilization as a bonding material in TEGs. Silver paste and the thermoelectric material interface is the most common place for defects such as micro cracks. Typically, a Ni barrier layer is applied on the surface of thermoelectric pellets to prevent silver diffusion inside the material. This barrier layer can be further investigated concerning the deposition method, thickness, and alternative materials to Ni.

- Another problem with silver is the cost issue, which could be replaced by developing cheaper sintering material in the future. Alternatively, electrically conductive adhesives (ECA) can be used for lower temperature ranges. These materials provide more mechanical flexibility and can be cured at lower temperature ranges. Still, the electrical conductivity is lower compared to the low-temperature solders, however, there is a great chance for future study of ECAs utilization in FTEGs.

- Most of the available silver sintering materials need to apply pressure to complete the sintering process, which adds complexity to the manufacturing process. Developing pressureless sintering materials that can compete with the former sintering materials can fully realize the high-speed automated assembly of the FTEGs.

- The proposed manufacturing platforms can also be tailored for the fabrication of other bulk thermoelectric materials instead of bismuth telluride. However, the bonding material and method should be adopted based on the behavior of each specific material.

- There are no robust industry scale specifications, test procedures, and standards for high throughput reliability tests and quality control of thermoelectric devices, which could be another area of research for fully scaling up the technology.

- Lige cycle management and recyclability of TEGs are other essential issues that need to be considered in any widespread application. Bismuth telluride TEGs contain both toxic and expensive rare earth elements. A whole life cycle management for FTEGs is necessary to reduce the potential negative environmental impacts and decrease the cost by using recycled materials.

LITERATURE LIST

[1]   G. J. Snyder and E. S. Toberer, "Complex TE meterials," *Nat. Mater.*, vol. 7, no. February, pp. 105–114, 2008.

[2]   T. J. Seebeck, "Ueber die magnetische Polarisation der Metalle und Erze durch Temperaturdifferenz [Magnetic polarization of metals and ores by temperature differences]," *Abhandlungen der K. Akad. der Wissenschaften zu Berlin (in Ger.*, 1826.

[3]   D. Rowe and B. Raton London New York, *Thermoelectrics Handbook*. CRC Press, 2018.

[4]   G. J. Snyder and E. S. Toberer, "Complex thermoelectric materials," *Nature Materials*, vol. 7, no. 2. Nature Publishing Group, pp. 105–114, Feb-2008.

[5]   D. Kraemer *et al.*, "High-performance flat-panel solar thermoelectric generators with high thermal concentration," *Nat. Mater.*, vol. 10, no. 7, pp. 532–538, 2011.

[6]   O. Beeri, O. Rotem, E. Hazan, E. A. Katz, A. Braun, and Y. Gelbstein, "Hybrid photovoltaic-thermoelectric system for concentrated solar energy conversion: Experimental realization and modeling," *J. Appl. Phys.*, vol. 118, no. 11, p. 115104, Sep. 2015.

[7]   F. Suarez, D. P. Parekh, C. Ladd, D. Vashaee, M. D. Dickey, and M. C. Öztürk, "Flexible thermoelectric generator using bulk legs and liquid metal interconnects for wearable electronics," *Appl. Energy*, vol. 202, pp. 736–745, Sep. 2017.

[8]   A. El-Desouky, M. Carter, M. A. Andre, P. M. Bardet, and S. LeBlanc, "Rapid processing and assembly of semiconductor thermoelectric materials for energy conversion devices," *Mater. Lett.*, vol. 185, pp. 598–602, Dec. 2016.

[9]   D. Lee *et al.*, "Liquid-metal-electrode-based compact, flexible, and high-power thermoelectric device," *Energy*, vol. 188, p. 116019, Dec. 2019.

[10]   Y. Eom, D. Wijethunge, H. Park, S. H. Park, and W. Kim, "Flexible thermoelectric power generation system based on rigid inorganic bulk materials," *Appl. Energy*, vol. 206, pp. 649–656, Nov. 2017.

[11]   F. Suarez, D. P. Parekh, C. Ladd, D. Vashaee, M. D. Dickey, and M. C. Öztürk, "Flexible thermoelectric generator using bulk legs and liquid metal interconnects for wearable electronics," *Appl. Energy*, vol. 202, pp. 736–745, Sep. 2017.

[12]   J. H. Bahk, H. Fang, K. Yazawa, and A. Shakouri, "Flexible thermoelectric materials and device optimization for wearable energy harvesting," *Journal of Materials Chemistry C*, vol. 3, no. 40. Royal Society of Chemistry, pp. 10362–10374, 08-Oct-2015.

[13]   O. Bubnova *et al.*, "Optimization of the thermoelectric figure of merit in the conducting polymer poly(3,4-ethylenedioxythiophene)," *Nat. Mater.*, vol. 10, no. 6, pp. 429–433, May 2011.

[14]   I. Petsagkourakis, K. Tybrandt, X. Crispin, I. Ohkubo, N. Satoh, and T. Mori, "Thermoelectric materials and applications for energy harvesting power generation," *Sci. Technol. Adv. Mater.*, vol. 19, no. 1, pp. 836–862, Dec. 2018.

[15]   A. Chen, D. Madan, P. K. Wright, and J. W. Evans, "Dispenser-printed planar thick-film thermoelectric energy generators," *J. Micromechanics Microengineering*, vol. 21, no. 10, p. 104006, Oct. 2011.

[16]   C. Navone, M. Soulier, M. Plissonnier, and A. L. Seiler, "Development of (Bi,Sb) 2(Te,Se) 3-based thermoelectric modules by a screen-printing process," *J. Electron. Mater.*, vol. 39, no. 9, pp. 1755–1759, Sep. 2010.

[17]   D. Madan, A. Chen, P. K. Wright, and J. W. Evans, "Dispenser printed composite thermoelectric thick films for thermoelectric generator applications," *J. Appl. Phys.*, vol. 109, no. 3, p. 034904, Feb. 2011.

[18]   R. R. Søndergaard, M. Hösel, N. Espinosa, M. Jørgensen, and F. C. Krebs, "Practical evaluation of organic polymer thermoelectrics by large-area R2R processing on flexible substrates," *Energy Sci. Eng.*, vol. 1, no. 2, pp. 81–88, Sep. 2013.

[19]   B. Russ, A. Glaudell, J. J. Urban, M. L. Chabinyc, and R. A. Segalman, "Organic thermoelectric materials for energy harvesting and temperature control," *Nat. Rev. Mater.*, vol. 1, no. 10, p. 16050, Aug. 2016.

[20]   Z. Lu *et al.*, "Fabrication of flexible thermoelectric thin film devices by inkjet printing," *Small*, vol. 10, no. 17. Wiley-VCH Verlag, pp. 3551–3554, 10-Sep-2014.

[21]   Y. Chen, Y. Zhao, and Z. Liang, "Solution processed organic thermoelectrics: Towards flexible thermoelectric modules," *Energy and Environmental Science*, vol. 8, no. 2. Royal Society of Chemistry, pp. 401–422, 01-Feb-2015.

[22]   S. Mortazavinatanzi, A. Rezaniakolaei, and L. Rosendahl, "Printing and Folding: A Solution for High-Throughput Processing of Organic Thin-Film Thermoelectric Devices," *Sensors 2018, Vol. 18, Page 989*, vol. 18, no. 4, p. 989, Mar. 2018.

[23]   D. Takemori, M. Okuhata, and M. Takashiri, "Thermoelectric Properties of Electrodeposited Bismuth Telluride Thin Films by Thermal Annealing and Homogeneous Electron Beam Irradiation," *ECS Trans.*, vol. 75, no. 52, pp. 123–131, Jan. 2017.

[24]   M. Yamaguchi, H. Yamamuro, and M. Takashiri, "Characteristics of electrodeposited bismuth telluride thin films with different crystal growth by adjusting electrolyte temperature and concentration," *Curr. Appl. Phys.*, vol. 18, no. 12, pp. 1513–1522, Dec. 2018.

[25]   Y. Sun *et al.*, "Low-Cost High-Performance Zinc Antimonide Thin Films for Thermoelectric Applications," *Adv. Mater.*, vol. 24, no. 13, pp. 1693–1696, Apr. 2012.

[26]   M. Mirhosseini, A. Rezania, A. B. Blichfeld, B. B. Iversen, and L. A. Rosendahl, "Experimental Investigation of Zinc Antimonide Thin Film Thermoelectric Element over Wide Range of Operating Conditions," *Phys. status solidi*, vol. 214, no. 11, p. 1700301, Nov. 2017.

[27]   M. S. Hossain, T. Li, Y. Yu, J. Yong, J. H. Bahk, and E. Skafidas, "Recent advances in printable thermoelectric devices: Materials, printing techniques, and applications," *RSC Advances*, vol. 10, no. 14. Royal Society of Chemistry, pp. 8421–8434, 26-Feb-2020.

[28]   J. Weber, K. Potje-Kamloth, F. Haase, P. Detemple, F. Völklein, and T. Doll,

"Coin-size coiled-up polymer foil thermoelectric power generator for wearable electronics," *Sensors Actuators, A Phys.*, vol. 132, no. 1 SPEC. ISS., pp. 325–330, Nov. 2006.

[29]   J. H. We, S. J. Kim, G. S. Kim, and B. J. Cho, "Improvement of thermoelectric properties of screen-printed Bi 2Te3 thick film by optimization of the annealing process," *J. Alloys Compd.*, vol. 552, pp. 107–110, Mar. 2013.

[30]   Z. Cao, E. Koukharenko, M. J. Tudor, R. N. Torah, and S. P. Beeby, "Flexible screen printed thermoelectric generator with enhanced processes and materials," *Sensors Actuators, A Phys.*, vol. 238, pp. 196–206, Feb. 2016.

[31]   T. Varghese *et al.*, "High-performance and flexible thermoelectric films by screen printing solution-processed nanoplate crystals," *Sci. Rep.*, vol. 6, no. 1, pp. 1–6, Sep. 2016.

[32]   H. Choi *et al.*, "UV-Curable Silver Electrode for Screen-Printed Thermoelectric Generator," *Adv. Funct. Mater.*, vol. 29, no. 20, p. 1901505, May 2019.

[33]   P. S. Chang and C. N. Liao, "Screen-printed flexible thermoelectric generator with directional heat collection design," *J. Alloys Compd.*, vol. 836, p. 155471, Sep. 2020.

[34]   T. Varghese *et al.*, "Flexible Thermoelectric Devices of Ultrahigh Power Factor by Scalable Printing and Interface Engineering," *Adv. Funct. Mater.*, vol. 30, no. 5, p. 1905796, Jan. 2020.

[35]   Q. Wei, M. Mukaida, K. Kirihara, Y. Naitoh, and T. Ishida, "Polymer thermoelectric modules screen-printed on paper," *RSC Adv.*, vol. 4, no. 54, pp. 28802–28806, Jun. 2014.

[36]   J. H. We, S. J. Kim, and B. J. Cho, "Hybrid composite of screen-printed inorganic thermoelectric film and organic conducting polymer for flexible thermoelectric power generator," *Energy*, vol. 73, pp. 506–512, Aug. 2014.

[37]   Z. Lu *et al.*, "Fabrication of Flexible Thermoelectric Thin Film Devices by Inkjet Printing," *Small*, vol. 10, no. 17, pp. 3551–3554, Sep. 2014.

[38]   B. Chen *et al.*, "Inkjet Printing of Single-Crystalline Bi 2 Te 3 Thermoelectric Nanowire Networks," *Adv. Electron. Mater.*, vol. 3, no. 4, p. 1600524, Apr. 2017.

[39]   B. Chen *et al.*, "Flexible thermoelectric generators with inkjet-printed bismuth telluride nanowires and liquid metal contacts," *Nanoscale*, vol. 11, no. 12, pp. 5222–5230, Mar. 2019.

[40]   A. Besganz, V. Zöllmer, R. Kun, E. Pál, L. Walder, and M. Busse, "Inkjet Printing as a Flexible Technology for the Deposition of Thermoelectric Composite Structures," *Procedia Technol.*, vol. 15, pp. 99–106, Jan. 2014.

[41]   S. Ferhat, C. Domain, J. Vidal, D. Noël, B. Ratier, and B. Lucas, "Organic thermoelectric devices based on a stable n-type nanocomposite printed on paper," *Sustain. Energy Fuels*, vol. 2, no. 1, pp. 199–208, Dec. 2018.

[42]   K. T. Park *et al.*, "High-performance thermoelectric bracelet based on carbon nanotube ink printed directly onto a flexible cable," *J. Mater. Chem. A*, vol. 6, no. 40, pp. 19727–19734, Oct. 2018.

[43]   M. Vaezi, H. Seitz, and S. Yang, "A review on 3D micro-additive manufacturing technologies," *International Journal of Advanced Manufacturing Technology*, vol.

67, no. 5–8. Springer London, pp. 1721–1754, 25-Nov-2013.

[44]   J. Yong *et al.*, "Fully Solution-Processed Transparent Artificial Neural Network Using Drop-On-Demand Electrohydrodynamic Printing," *ACS Appl. Mater. Interfaces*, vol. 11, no. 19, pp. 17521–17530, May 2019.

[45]   D. Madan, Z. Wang, A. Chen, R. Winslow, P. K. Wright, and J. W. Evans, "Dispenser printed circular thermoelectric devices using Bi and Bi 0.5Sb1.5Te3," *Appl. Phys. Lett.*, vol. 104, no. 1, p. 013902, Jan. 2014.

[46]   D. Madan *et al.*, "Enhanced performance of dispenser printed MA n-type Bi2Te 3 composite thermoelectric generators," *ACS Appl. Mater. Interfaces*, vol. 4, no. 11, pp. 6117–6124, Nov. 2012.

[47]   D. Madan, Z. Wang, P. K. Wright, and J. W. Evans, "Printed flexible thermoelectric generators for use on low levels of waste heat," *Appl. Energy*, vol. 156, pp. 587–592, Oct. 2015.

[48]   K. Wu *et al.*, "Preparation of n-type Bi $_2$ Te $_3$ thermoelectric materials by non-contact dispenser printing combined with selective laser melting," *Phys. status solidi - Rapid Res. Lett.*, vol. 11, no. 6, p. 1700067, Jun. 2017.

[49]   S. E. Jo, M. K. Kim, M. S. Kim, and Y. J. Kim, "Flexible thermoelectric generator for human body heat energy harvesting," *Electron. Lett.*, vol. 48, no. 16, pp. 1015–1017, Aug. 2012.

[50]   C. Ou, A. L. Sangle, T. Chalklen, Q. Jing, V. Narayan, and S. Kar-Narayan, "Enhanced thermoelectric properties of flexible aerosol-jet printed carbon nanotube-based nanocomposites," *APL Mater.*, vol. 6, no. 9, p. 096101, Sep. 2018.

[51]   M. Saeidi-Javash, W. Kuang, C. Dun, and Y. Zhang, "3D Conformal Printing and Photonic Sintering of High-Performance Flexible Thermoelectric Films Using 2D Nanoplates," *Adv. Funct. Mater.*, vol. 29, no. 35, p. 1901930, Aug. 2019.

[52]   C. T. Hong, Y. H. Kang, J. Ryu, S. Y. Cho, and K. S. Jang, "Spray-printed CNT/P3HT organic thermoelectric films and power generators," *J. Mater. Chem. A*, vol. 3, no. 43, pp. 21428–21433, Oct. 2015.

[53]   "Thermoelectric Thin Films - Materials and Devices | Paolo Mele | Springer." [Online]. Available: https://www.springer.com/gp/book/9783030200428. [Accessed: 20-Aug-2020].

[54]   B. Geun Kim, S. Hyun Bae, J. Byeon, C. Lee, and S. M. Choi, "Stress-induced change of Cu-doped Bi2Te3 thin films for flexible thermoelectric applications," *Mater. Lett.*, vol. 270, p. 127697, Jul. 2020.

[55]   Z. Cai *et al.*, "Bi-Sb-Te based thin film thermoelectric generator," in *Advanced Materials Research*, 2012, vol. 538–541, pp. 60–63.

[56]   D. Kong, W. Zhu, Z. Guo, and Y. Deng, "High-performance flexible Bi2Te3 films based wearable thermoelectric generator for energy harvesting," *Energy*, vol. 175, pp. 292–299, May 2019.

[57]   S. Kianwimol, P. Wanarattikan, R. Sakdanuphab, P. Pluengphon, T. Bovornratanaraks, and A. Sakulkalavek, "Experimental Study on Flexible Bismuth Telluride Thin Films Deposited by DC Sputtering at Different Powers," *J. Electron. Mater.*, vol. 48, no. 6, pp. 3490–3496, Jun. 2019.

[58]   P. Fan *et al.*, "The high performance of a thin film thermoelectric generator with

heat flow running parallel to film surface," *Appl. Phys. Lett.*, vol. 102, no. 3, p. 033904, Jan. 2013.

[59]   P. Fan *et al.*, "Low-cost flexible thin film thermoelectric generator on zinc based thermoelectric materials," *Appl. Phys. Lett.*, vol. 106, no. 7, p. 073901, Feb. 2015.

[60]   G. J. Snyder, J. R. Lim, C. K. Huang, and J. P. Fleurial, "Thermoelectric microdevice fabricated by a MEMS-like electrochemical process," *Nature Materials*, vol. 2, no. 8. European Association for Cardio-Thoracic Surgery, pp. 528–531, 27-Jul-2003.

[61]   D. W. Liu and J. F. Li, "Microfabrication of thermoelectric modules by patterned electrodeposition using a multi-channel glass template," *J. Solid State Electrochem.*, vol. 15, no. 3, pp. 479–484, Mar. 2011.

[62]   K. Matsuoka, M. Okuhata, N. Hatsuta, and M. Takashiri, "Effect of composition on the properties of bismuth telluride thin films produced by galvanostatic electrodeposition," *Trans. Mater. Res. Soc. Japan*, vol. 40, no. 4, pp. 383–387, Dec. 2015.

[63]   K. Matsuoka, M. Okuhata, and M. Takashiri, "Dual-bath electrodeposition of n-type Bi-Te/Bi-Se multilayer thin films," *J. Alloys Compd.*, vol. 649, pp. 721–725, Aug. 2015.

[64]   M. Takashiri, T. Makioka, and H. Yamamuro, "Promotion of crystal growth in as-grown Bi2Te3 electrodeposited films without micro-pores using sputtered Bi2Te3 seed layers deposited on a glass substrate," *J. Alloys Compd.*, vol. 764, pp. 802–808, Oct. 2018.

[65]   K. Yamauchi, R. Mori, M. Yamaguchi, and M. Takashiri, "Thermoelectric properties including thermal conductivity of electrodeposited bismuth selenide thin films fabricated using different acid solutions," *J. Alloys Compd.*, vol. 792, pp. 222–229, Jul. 2019.

[66]   N. Su, S. Guo, F. Li, and B. Li, "Electrodeposition of Bi-Te Thin Films on Silicon Wafer and Micro-Column Arrays on Microporous Glass Template," *Nanomaterials*, vol. 10, no. 3, p. 431, Feb. 2020.

[67]   Y. Wang, Y. Shi, D. Mei, and Z. Chen, "Wearable thermoelectric generator to harvest body heat for powering a miniaturized accelerometer," *Appl. Energy*, vol. 215, pp. 690–698, Apr. 2018.

[68]   Y. Sargolzaeiaval *et al.*, "Flexible thermoelectric generators for body heat harvesting – Enhanced device performance using high thermal conductivity elastomer encapsulation on liquid metal interconnects," *Appl. Energy*, vol. 262, p. 114370, Mar. 2020.

[69]   H. Park *et al.*, "Mat-like flexible thermoelectric system based on rigid inorganic bulk materials," *J. Phys. D. Appl. Phys.*, vol. 50, no. 49, p. 494006, Nov. 2017.

[70]   H. Park *et al.*, "High power output from body heat harvesting based on flexible thermoelectric system with low thermal contact resistance," *J. Phys. D. Appl. Phys.*, vol. 51, no. 36, p. 365501, Aug. 2018.

[71]   Y. Wei, R. Torah, K. Yang, S. Beeby, and J. Tudor, "Screen printing of a capacitive cantilever-based motion sensor on fabric using a novel sacrificial layer process for smart fabric applications," *Meas. Sci. Technol.*, vol. 24, no. 7, pp. 75104–75115,

Jun. 2013.

[72]   S. Shin *et al.*, "High-Performance Screen-Printed Thermoelectric Films on Fabrics," *Sci. Rep.*, vol. 7, no. 1, pp. 1–9, Dec. 2017.

[73]   R. Chierchia, E. Salza, and A. Mittiga, "Effect of Hydrogen gas dilution on sputtered Al:ZnO film," *Energy Procedia*, vol. 60, no. C, pp. 135–142, Jan. 2014.

[74]   S. Mortazavinatanzi, S. Mojtaba Mir Hosseini, L. Song, B. Brummerstedt Iversen, L. Rosendahl, and A. Rezania, "Zinc Antimonide Thin Film Based Flexible Thermoelectric Module," *Mater. Lett.*, vol. 280, p. 128582, Aug. 2020.

[75]   S. Mortazavinatanzi, A. Rezaniakolaei, and L. Rosendahl, "High-throughput Manufacturing of Flexible Thermoelectric Generators for Low to Medium Temperature Applications Based on Nano-silver Bonding," *IEEE Trans. Electron Devices*, no. submitted, 2020.

[76]   A. Stranz, A. Waag, and E. Peiner, "Investigation of Thermoelectric Parameters of Bi2Te3: TEGs Assembled using Pressure-Assisted Silver Powder Sintering-Based Joining Technology," *J. Electron. Mater.*, vol. 44, no. 6, pp. 2055–2060, Jun. 2015.

[77]   J. G. Bai and G. Q. Lu, "Thermomechanical reliability of low-temperature sintered silver die attached SiC power device assembly," *IEEE Trans. Device Mater. Reliab.*, vol. 6, no. 3, pp. 436–441, Sep. 2006.

[78]   W. Guo, Z. Zeng, X. Zhang, P. Peng, and S. Tang, "Low-temperature sintering bonding using silver nanoparticle paste for electronics packaging," *J. Nanomater.*, vol. 2015, 2015.

[79]   Y. Morisada, T. Nagaoka, M. Fukusumi, Y. Kashiwagi, M. Yamamoto, and M. Nakamoto, "A low-temperature bonding process using mixed Cu-Ag nanoparticles," *J. Electron. Mater.*, vol. 39, no. 8, pp. 1283–1288, Aug. 2010.

[80]   P. Peng, A. Hu, H. Huang, A. P. Gerlich, B. Zhao, and Y. N. Zhou, "Room-temperature pressureless bonding with silver nanowire paste: Towards organic electronic and heat-sensitive functional devices packaging," *J. Mater. Chem.*, vol. 22, no. 26, pp. 12997–13001, Jul. 2012.

[81]   A. Rezania and E. Yazdanshenas, "Effect of substrate layers on thermo-electric performance under transient heat loads," *Energy Convers. Manag.*, vol. 219, p. 113068, Sep. 2020.